Protein-protein-interaction Network Organization of the Hypusine Modification System*⑤

Henning Sievert‡[a], Simone Venz§[a], Oscar Platas-Barradas¶, Vishnu M. Dhople‖, Martin Schaletzky¶, Claus-Henning Nagel, Melanie Braig‡, Michael Preukschas‡, Nora Pällmann‡, Carsten Bokemeyer‡, Tim H. Brümmendorf‡‡, Ralf Pörtner¶, Reinhard Walther§, Kent E. Duncan§§, Joachim Hauber**, and Stefan Balabanov‡¶¶‖‖**

Hypusine modification of eukaryotic initiation factor 5A (eIF-5A) represents a unique and highly specific post-translational modification with regulatory functions in cancer, diabetes, and infectious diseases. However, the specific cellular pathways that are influenced by the hypusine modification remain largely unknown. To globally characterize eIF-5A and hypusine-dependent pathways, we used an approach that combines large-scale bioreactor cell culture with tandem affinity purification and mass spectrometry: "bioreactor-TAP-MS/MS." By applying this approach systematically to all four components of the hypusine modification system (eIF-5A1, eIF-5A2, DHS, and DOHH), we identified 248 interacting proteins as components of the cellular hypusine network, with diverse functions including regulation of translation, mRNA processing, DNA replication, and cell cycle regulation. Network analysis of this data set enabled us to provide a comprehensive overview of the protein-protein interaction landscape of the hypusine modification system. In addition, we validated the interaction of eIF-5A with some of the newly identified associated proteins in more detail. Our analysis has revealed numerous novel interactions, and thus provides a valuable resource for understanding how this crucial homeostatic signaling pathway affects different cellular functions.   *Molecular & Cellular Proteomics* 11: 10.1074/mcp.M112.019059, 1289–1305, 2012.

Cellular homeostasis is controlled by signaling networks that communicate through post-translational modifications (PTM)[1] of proteins, including phosphorylation, acetylation and methylation (1–3). These modifications are typically attached to various types of proteins by multiple independent enzymes, and thereby simultaneously regulate a wide range of protein functions. Consequently, most signaling pathways are highly redundant, enabling maintenance of cellular integrity even if the modification of a single signaling molecule is disrupted (4). A striking exception is hypusine. This essential PTM is limited to a single protein: the eukaryotic initiation factor 5A (eIF-5A) (5). Disruption of this PTM leads to growth arrest in proliferating eukaryotic cells and is fatal for the developing mammalian embryo (6, 7). During hypusine biosynthesis, the lysine residue at position 50 (Lys_{50}) in eIF-5A is converted into the unusual amino acid hypusine (N^ε-(4-amino-2-hydroxybutyl)lysine; depicted in Fig. 1A) (5). This process activates eIF-5A and is mediated by two enzymatic reactions: first, deoxyhypusine synthase (DHS) catalyzes the transfer of the 4-aminobutyl moiety of spermidine to the ε-amino group of Lys_{50} to form an intermediate residue, deoxyhypusine (Dhp_{50}) (8). Subsequently, deoxyhypusine hydroxylase (DOHH) mediates the

From the ‡Department of Oncology, Hematology and Bone Marrow Transplantation with Section Pneumology, Hubertus Wald-Tumor Zentrum, University Hospital Eppendorf, Hamburg, Germany; §Department of Medical Biochemistry and Molecular Biology, University of Greifswald, Greifswald, Germany; ¶Institute of Bioprocess and Biosystems Engineering, Hamburg University of Technology, Hamburg, Germany; ‖Interfaculty Institute for Genetics and Functional Genomics, Department of Functional Genomics, Ernst-Moritz-Arndt-University of Greifswald, Greifswald, Germany; **Heinrich-Pette-Institute - Leibniz Institute for Experimental Virology, Hamburg, Germany; ‡‡Clinic for Internal Medicine IV, Hematology and Oncology, University Hospital of the RWTH Aachen, Aachen, Germany; §§Neuronal Translational Control Group, Center for Molecular Neurobiology, ZMNH, University of Hamburg Medical School, Hamburg, Germany; ¶¶Division of Hematology, University Hospital Zurich, Zurich, Switzerland

[1] The abbreviations used are: PTM, post-translational modification; BCR-ABL, fusion protein of 'breakpoint cluster region' and 'proto-oncogene c-Abl'; Cer2, Cerulian 2; DHS, deoxyhypusine synthase; DOHH, deoxyhypusine hydroxylase; eGFP, enhanced green fluorescent protein; eIF-5A, eukaryotic initiation factor 5A; ESCRT-I, endosomal sorting complexes required for transport-I; FTICR, Fourier transform ion cyclotron resonance mass spectrometry; GC7, N1-guanyl-1,7-diaminoheptane (Inhibitor of DHS); GO, gene ontology; HIV, human immunodeficiency virus; HMS, hypusine modification system; LeGO, lentiviral gene ontology vectors; MVB, multivesicular bodies; mRFP, monomeric red fluorescent protein; mRNA, messenger RNA; PCA, protein fragment complementation assay; PPI, protein-protein interaction; TAP, tandem affinity purification; YFP, yellow fluorescent protein.

formation of hypusine (Hyp_{50}) by addition of a hydroxyl group to the deoxyhypusine residue (9). eIF-5A, DHS and DOHH are all essential for proliferation of higher eukaryotic cells (10, 11), and eIF-5A is strictly conserved throughout eukaryotic evolution (12).

The eIF-5A protein has been proposed to promote various different cellular processes that potentially regulate proliferation, including translation initiation (13) and elongation (14) as well as nucleocytoplasmic transport of RNA or other cargoes (15, 16). Using inhibitors of DHS and DOHH or eIF-5A mutants deficient for hypusine modification, it has also been shown that this modification is a prerequisite of at least a subset of known eIF-5A functions (10, 11, 17, 18). The eIF-5A protein has also been implicated in numerous pathologic conditions including various types of cancer (19–23), β-cell inflammation (and therefore diabetes) (24) and HIV-1 infection (25). Human and rodent cells carry two highly homologous eIF-5A genes coding for distinct isoforms. Although eIF-5A1 is expressed at high levels throughout all tissues, eIF-5A2 is detectable only in a few embryonic tissues as well as adult testis, central nervous system (26), and cancer tissue (21, 22, 27–29).

Although there have been ample reports suggesting eIF-5A is involved in translational control, the molecular mechanisms through which it ultimately influences cellular physiology and leads to disease remain unclear. Moreover, it remains equally possible that at least some of eIF-5A's effects on cellular functions might not involve direct effects on translation. Also, there is no information available on whether the two isoforms of mammalian eIF-5A are functionally congruent.

To address these fundamental questions systematically and comprehensively, we employed a bioreactor-based tandem affinity purification (TAP) approach followed by MS identification of purified protein complexes ("bioreactor-TAP-MS/MS"). To obtain a complete interaction map of the proteins involved in hypusine modification, we used this approach to identify interaction partners of both isoforms of eIF-5A, as well as the hypusine modification enzymes DHS and DOHH. In total, we identified 248 proteins that either directly interact with these bait proteins or are components of higher complexes containing the aforementioned proteins. Furthermore, we validated a subset of putative interaction partners of both eIF-5A isoforms, using Western blots of reciprocal TAP experiments, as well as a live-cell protein-fragment complementation assay (PCA). Our analysis provides a molecular framework for a detailed understanding on how this signal transduction pathway affects different crucial cellular functions.

EXPERIMENTAL PROCEDURES

Cloning of Plasmid Constructs—A retroviral pCeMM expression plasmid encoding a C-terminal SG-tag was kindly provided by Prof. Superti-Furga, Vienna, A, (30); pcDNA3 expression plasmids containing the MCFD2 insert, C-terminally fused to YFP_1 and YFP_2 fragments, were kindly provided by Prof. H.-P. Hauri, Basel, CH (31); and an expression plasmid encoding LC3 protein N-terminally fused to monomeric red fluorescent protein (mRFP-LC3) (32, 33) was obtained

from Addgene, Cambridge, MA. To generate more versatile cloning vectors for the protein fragment complementation assay (PCA), the tag sequences were PCR-amplified from the plasmid DNA and cloned into empty pcDNA3 plasmid as described above, thereby including a new multiple cloning site. The LC3 sequence of mRFP-LC3 was exchanged for cDNA sequences of calreticulin (NM_007591), Dcp1a (NM_133761), TIA-1 (NM_011585), and TSG101 (NM_021884). The N-terminal mRFP tag sequences were subsequently removed and the sequence coding for Cerulian 2 (Cer2) inserted into the plasmid (a LeGO plasmid encoding Cer2 was a kind gift of Prof. B. Fehse, Hamburg, D). All plasmids were built using standard RT-PCR- and restriction-enzyme based cloning. The TAP- and PCA-constructs used in this study are provided in supplemental Table S5. Point mutants coding for all eIF-5A$_{K50R}$ and $_{G52A}$ mutants were generated using the Phusion site directed mutagenesis kit (Finnzymes, Vantaa, Finland).

Cell Culture—NIH3T3 were cultivated in Dulbecco's modified Eagle's medium (DMEM) + GlutMAX-I supplemented with 10% fetal bovine serum, 100 U/ml penicillin and 100 μg/ml streptomycin. Vero cells (ATCC-CCL81, kidney epithelial cells from *Cercopithecus aethiops*) were cultivated in Dulbecco's modified Eagle's medium supplemented with 10% fetal bovine serum. Ba/F3 cells expressing oncogenic Bcr-Abl (Ba/F3 p210; kindly provided by Prof. C. L. Sawyers, Los Angeles, CA) were cultivated in RPMI 1640 + GlutaMAX-I supplemented with 10% fetal bovine serum, 1 mM sodium pyruvate, 1× MEM nonessential amino acids, 100 U/ml penicillin and 100 μg/ml streptomycin. All Media and supplements from Invitrogen (Invitrogen, Darmstadt, Germany). All cells were incubated at 37 °C, 5% CO_2 and 95% relative humidity.

Bioreactor-based Tandem Affinity Purification (bioreactor-TAP)—To establish stable bait expressing cell lines, separate retroviral transductions of the Ba/F3 p210 cell line were performed with each pCeMM construct. Retroviral transduction was carried out as described before (23, 34). To ensure constant cell culture conditions, we decided to employ bioreactor based cell cultivation rather than flask-based cell culture. This approach enabled us to generate high numbers of cells and maintain constant and reproducible culture conditions (35). Because of the high reproducibility of separate reactor runs, we decided to split samples of reactor-cultured cells after lysis, thus providing technical replicates of the more error-prone downstream processes. This approach was applied to the following bait proteins: eIF-5A1, eIF-5A2, DHS, DOHH, and eGFP (providing the bead proteome control dataset). The TAP procedure was adapted from Bürckstümmer *et al.* (30). In short, up to 10^{10} cells expressing one of the bait proteins were washed in PBS and lysed 15 min in 50 mM Tris at pH 7.6 containing 125 mM NaCl, 5% glycerol, 0.2% Nonidet P-40, 1.5 mM $MgCl_2$, 25 mM NaF, 1 mM Na_3VO_4, and 1x protease inhibitor mixture (Sigma). The lysate was cleared (48,000 × *g*, 45 min). Supernatants of scale-up experiments for mass spectrometric identification were now split into two separately handled fractions. The supernatant was incubated with IgG-beads (GE Healthcare, Uppsala, Sweden) for 2 h, and the beads washed three times with lysis buffer and three times with TEV reaction buffer (10 mM Tris at pH 7.6, 100 mM NaCl, 0.2% Nonidet P-40, and 0.5 mM EDTA). The SG-tag was cleaved by incubation with acTEV protease (Invitrogen, Carlsbad, CA) for 3 h, directly followed by incubation of the supernatant with streptavidin beads (Thermo Scientific) for 1 h. The beads were washed three times and the bound protein complexes eluted by boiling in SDS lysis buffer (50 mM Tris-HCl, pH 7.6 containing 150 mM NaCl, 1% Nonidet P-40, 0.25% Na-desoxycholate, and 1× protease inhibitor mixture). Eluates for mass spectrometry were separated by 1D-PAGE over a length of 2 to 4 cm. Gels were stained using RotiBlue (Carl Roth, Karlsruhe, Germany) and sliced into 8 to 10 samples per replicate.

³H-labeled Spermidine Incorporation Assay—Incorporation of ³H-labeled spermidine into the hypusine modification of eIF-5A was quantified as described in detail by Wolff *et al.* (36, 37).

Mass Spectrometry—Proteins were digested in-gel using 10 ng/µl trypsin in 20 mM ammonium bicarbonate and incubated at 37 °C overnight, followed by peptide extraction with 50% acetonitrile containing 0.1% acetic acid. The supernatants were dried and peptides were dissolved in 10 µl buffer containing 0.1% acetic acid and 2% acetonitrile. The peptide solutions were analyzed either using a FTICR mass spectrometer (Finnigan LTQ FT, Thermo Electron Corp.) coupled to a nanoACQUITY Ultra Performance LC (UPLC) (Waters Corp., Milford, MA) and controlled by Xcalibur software (Thermo Electron Corp) or using a Proxeon Easy nLC (Proxeon Biosystems A/S, Denmark) connected to a LTQ-Orbitrap XL (Thermo Electron Corp.) and equipped with a nano-ESI source.

In detail, the peptides for FTICR measurements were enriched on a nanoACQUITY Symmetry C18 pre-column (2 cm length, 180 µm inner diameter and 5 µm particle size, Waters Corp.) and separated using NanoAcquity BEH130 C18 column (10 cm length, 100 µM inner diameter and 1.7 µm particle size, Waters Corp.) on a nanoACQUITY UPLC. The separation was achieved with the formation of a linear gradient of 92 min containing buffer A (2% acetonitrile in water with 0.1% acetic acid) and buffer B (acetonitrile with 0.1% acetic acid, gradient-1–5% buffer B in 2 min, 5–25% B in 63 min, 25–60% B in 25 min, 60–99% B in 2 min). The peptides were eluted at a flow rate of 400 nl/min and analyzed using FTICR mass spectrometer with a nano-ESI source. The full scan was carried out using FTMS analyzer with normal mass range of *m/z* 400–1500. The data was acquired in profile mode with a resolution of 50,000 and positive polarity. This was followed by data dependent acquisition of top five intense precursor ions for MS/MS scans using CID activation. A minimum of 1000 counts were activated for 30 ms with an activation of q = 0.25 and a normalized collision energy of 35%. The charge state screening and monoisotopic precursor selection was enabled with the rejection of +1 and unassigned charge states. The peptides were excluded for the next 60 s once they were subjected to MS/MS scans.

For the measurements on the LTQ Orbitrap XL mass spectrometer, the peptides were separated using Proxeon Easy nLC and an Acclaim PepMap 100 analytical column (C18, particle size 3 µm, bed length 15 cm, 100 Å, LC-Packings, Dionex, Sunnyvale, CA). The peptides were enriched on a Biosphere C18 pre-column (ID 100 µM, particle size 5 µm, length 20 mm, pore size 120 Å, NanoSeparations, NL). The peptides were eluted at a flow rate of 300 nl/min with formation a solvent gradient of Buffer A and B (1–2% buffer B in 1 min, 2–25% B in 59 min, 25–40% B in 10 min, 40–100% B in 5 min). The buffer composition of A and B were same as used for UPLC. The MS was operated in data-dependent mode to automatically switch between Orbitrap-MS and LTQ-MS/MS acquisition. Survey full scan MS spectra (from *m/z* 400 to 1500) were acquired in the Orbitrap with resolution *r* = 60,000. The method used allowed sequential isolation of up to five of the most intense ions, depending on signal intensity and for fragmentation on the linear ion trap using collision-induced dissociation. Target ions already selected for MS/MS were dynamically excluded for 60 s. General MS conditions were 1.6 kV electrospray voltage with no sheath and auxiliary gas flow. Ion selection threshold was 1000 counts for MS/MS; an activation Q-value of 0.25 and activation time of 30 ms were also applied for MS/MS.

Protein identification was performed by automated database searches using the Sequest algorithm rel. 27.11 (Sorcerer built 4.04, Sage-N Research Inc., Milpitas, CA) and the Swiss-Prot database rel. 57.15 (forward-reverse, limited to 32448 mouse entries). The considered enzyme specificity was fully tryptic allowing two missed cleav-

ages. Parent and fragment mass tolerance (MS) were set to 10 ppm and 1 Da, respectively. Methionine oxidation and carbamidomethylation (on C) were considered as optional modification. Protein identification was based on a) peptide thresholds, with a 95.0% confidence minimum, Sequest: ΔCn scores of greater than 0.4, and XCorr scores of greater than 2.0 or 3.5 for doubly and triply charged peptides, respectively; and b) protein thresholds, with 95.0% confidence and two peptides identification minima.

Bioinformatic Evaluation of Identified PPI for the HMS—The resulting identifications for each bait protein were filtered for proteins that were identified in both technical replicates. Hits flagged as bead proteome were also removed from each data set. The adjusted lists were combined into one spoke interaction map using Cytoscape 2.8.1 (38). Furthermore, the network was enriched by using IPA 9.0 (Ingenuity Systems, Redwood City, CA) and Uniprot (39) to annotate function and subcellular localization for the prey proteins. The datasets were uploaded to STRING 9.0 (40) and IntAct 3.1 (41) databases to interconnect network nodes by adding previously reported interactions. The ClusterONE Cytoscape plugin 0.92 (42) was used to identify significantly interconnected clusters of nodes in the final interaction map. The PANTHER database 7.0 (43, 44) was used for gene ontology analysis, whereas bacterial/yeast/mammalian orthologs of proteins were queried from the OMA browser (45).

Western Blotting—All Western blot analysis was performed as described previously (46, 47). The employed antibodies were rabbit anti-eIF-5A1 (Novus Biologicals, Littleton, CA), rabbit anti-Myc-tag (Cell Signaling, Boston, MA), and anti-rabbit-HRP (Cell Signaling).

Protein Fragment Complementation Assay (PCA)—3T3 cells were seeded the day before transfection at a density of 10⁵ cells per well in 24-well format and transfected using Lipofectamin 2000 (Invitrogen, Carlsbad, CA) according to manufacturer's instructions, with a total of 3 µg plasmid DNA and 6 µl transfection reagent per well. Fluorescence-microscopic and flow cytometric analyses were carried out 24 h after transfection, recording mean fluorescence values of whole viable cell populations. Fluorescence microscopy was carried out using an IX81 fluorescence microscope equipped with a U-RFL-T high pressure mercury burner (Olympus, Tokyo, Japan). Quantitative analysis was carried out using a FACSCalibur flow cytometer (BD, Franklin Lakes, NJ).

Fluorescence Microscopy and Immunolabeling of PCA-transfected Cells—Vero cells (ATCC-CCL81, kidney epithelial cells from *Cercopithecus aethiops*) were seeded onto 10 mm cover slips in 24-well plates at 1 × 10⁵ cells/well and the next day transfected with 0.5 µg plasmid DNA per well (0.25 µg each of pcDNA3 eIF-5A1-YFP₁ and pcDNA3 DHS-YFP₂) using TransIT LT1 (Mirus Bio, Madison, WI). One day after transfection, the cells were fixed with 3% PFA in PBS containing calcium and magnesium for 20 min. PFA was quenched by washing with 50 mM NH₄Cl in PBS and the cells were permeabilized with 0.1% Triton X-100 in PBS for 5 min. After blocking with 0.5% bovine serum albumin in PBS, immunolabeling was performed with anti-calreticulin or anti-EEA1 (both Abcam, Cambridge, MA). Secondary antibodies were coupled to Alexa633 (Invitrogen, Grand Island, NY). The specimens were analyzed on an Axiovert 200 M microscope equipped with an LSM 510 META confocal laser scanning unit (Zeiss, Jena, Germany) using a Plan-Apochromatic ×63 oil immersion objective lens with a 1.4 numeric aperture. Image acquisition and processing was performed by using the Zeiss LSM imaging software and Adobe Photoshop CS3 (Adobe Systems, San Jose, CA).

Statistical Analysis—All PCA combinations were carried out in parallel duplicates paired with appropriate controls. Runs were independently reproduced to a total n of 4 wells per combination and all values analyzed using one-way ANOVA repeated measures test, with Dunnett or Bonferroni post tests applied where appropriate, as all combinations were compared with the respective MCFD2 negative
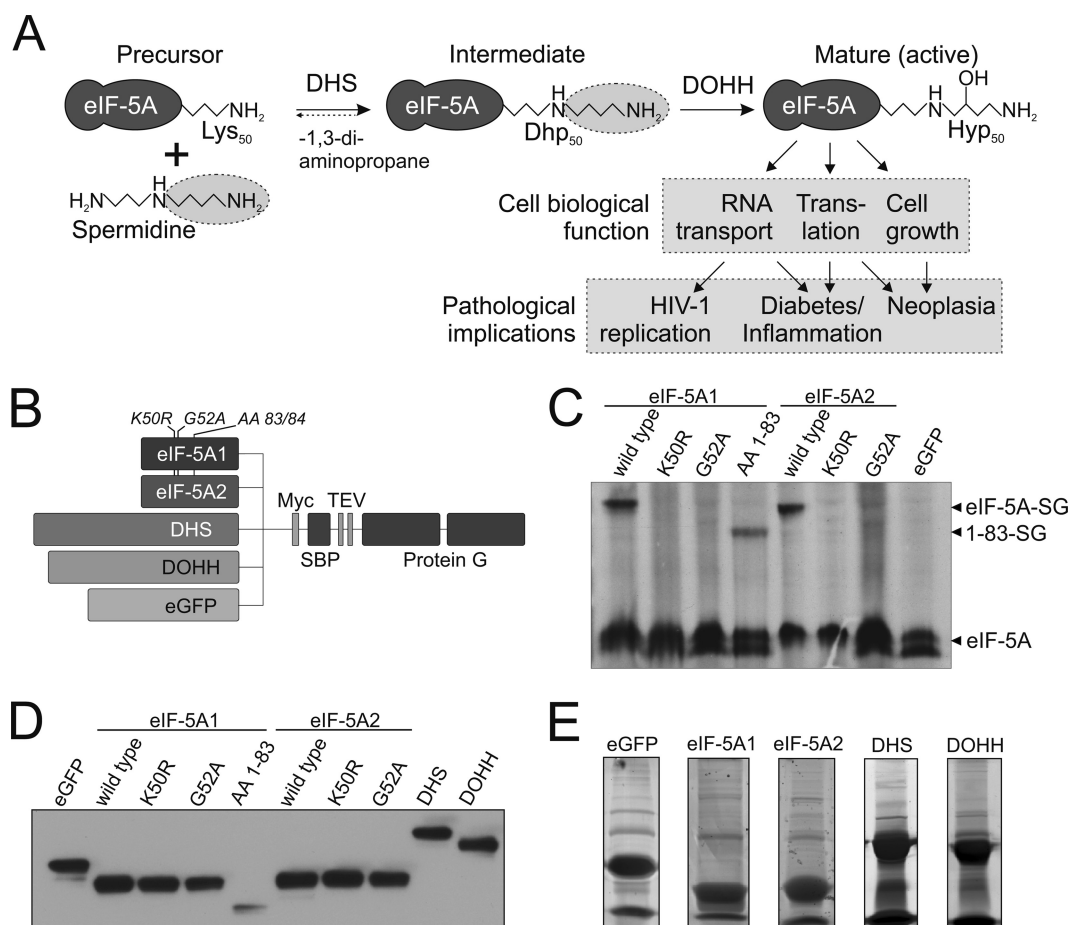
FIG. 1. **The hypusine modification and TAP fusion proteins employed in this study.** *A*, The hypusine modification pathway and major proposed eIF-5A functions. *B*, Structure of the plasmid inserts coding for SG-tagged bait proteins. The amino acid positions of eIF-5A mutants are indicated in italic. SBP, streptavidin binding peptide. *C*, Metabolic incorporation of ^{3}H-labeled spermidine into eIF-5A. Arrowheads indicate bands of SG-tagged and endogenous eIF-5A proteins. *D*, Anti-Myc-tag Western blot of cell lysates from retrovirally transduced Ba/F3 p210 cell lines for the quantification of constitutively expressed SG-tagged bait proteins. *E*, Representative TAP outputs for MS/MS analysis, after 1D PAGE separation and Coomassie staining. Separation distance varies from ~2 to 4 cm.

control and/or all other wild type and mutant forms of the same protein. Differences of mean fluorescence values normalized to the MCFD2 negative control with $p < 0.05$ were considered statistically relevant. Significances are represented with asterisks (*), with * for $p < 0.05$, ** for $p < 0.01$, and *** for $p < 0.001$. Diagrams of PCA experiments show means of fluorescence values (columns) and standard error of the mean (S.E., error bars).

RESULTS

Detection of Protein-protein Interactions of the Hypusine Modification System Using Bioreactor-TAP-MS/MS—A schematic overview of the workflow described in this manuscript is presented in supplemental Fig. S1. The HMS proteins were tagged with a streptavidin-IgG-tag (SG) and stably expressed via pCeMM (30) expression vectors (Fig. 1*B*). C-terminal tagging was chosen as N-terminal tags impede the hypusine modification of eIF-5A. To investigate the effect of the hypusine modification on newly identified PPI, we also constructed two mutant forms of eIF-5A: The Arg-substitution of Lys$_{50}$, the residue that is used for hypusine biosynthesis, as

well as the substitution of Gly$_{52}$ by Ala. Importantly, both eIF-5A$_{K50R}$ and eIF-5A$_{G52A}$ mutations prevent the biosynthesis of hypusine (48). To enable mapping of newly identified PPI to distinct domains of eIF-5A, two deletion mutants (eIF-5A$_{1-83}$ and eIF-5A$_{84-154}$) were also cloned, representing the functionally and structurally distinct N- and C-terminal domains of this protein (49) (Fig. 1*B*). A ^{3}H-spermidine incorporation assay (50) demonstrated that both eIF-5A1 (SG) and eIF-5A2 (SG), as well as the eIF-5A$_{1-83}$ (SG) deletion mutants, displayed efficient incorporation of ^{3}H-spermidine, as compared with the hypusine-modification deficient mutants (Fig.1*C*).

As shown by Western blot, we obtained robust constitutive expression of SG-tagged bait proteins eIF-5A1, eIF-5A2, DHS, DOHH, and eGFP at comparable levels (Fig. 1*D*). Maintenance of optimal and standardized conditions during cell expansion is a prerequisite for reliable, reproducible, and comparable results; particularly because many PPI are highly dynamic depending on the conditions of both the intra- and

extracellular environment. Flask-based cell culture does not allow for monitoring and constant adjustment of crucial culture conditions like medium pH or glucose concentration. Therefore, the generation of reliable and reproducible PPI networks is usually accomplished by analyzing biological replicates from independent flask-based cell cultures. To optimize cell culture conditions and reproducibility of downstream processes, we used a 5 L bioreactor for the rapid production of Ba/F3 p210 suspension cells expressing the respective bait protein, rather than flask-based cell culture. The rationale for using Ba/F3 p210 cells was that we have previously shown eIF-5A to exert a specific effect on chronic myeloid leukemia (23), for which this cell line is an established model system. As shown in supplemental Fig. S2, the bioreactor enabled the monitoring and adjustment of medium pH and dissolved oxygen at regular intervals. Additionally, yields of up to 10^{10} cells were achieved as starting material for the TAP assay without reaching glucose limitation. Taken together, these factors ensured optimal and reproducible conditions for cell culture. The monitoring of key parameters also revealed high comparability of the different reactor runs. We therefore concluded that preparing technical replicates of the TAP-MS/MS workflow from one batch of cells grown under the same conditions in the bioreactor, in contrast with producing flask-based biological replicates, would be a valid approach with regard to reproducibility. Coomassie staining of bioreactor-TAP outputs separated by 1D SDS-PAGE revealed striking differences in the protein band patterns for different bait proteins, suggesting that specific interactions were readily detectable using this approach (Fig. 1*E*).

Two complementary control experiments to validate putative novel interaction partners were implemented: First, all proteins that copurified with eGFP (SG) were flagged as bead proteome to identify false positive interaction partners (51, 52). Second, cell lysates were split in two equal samples and handled separately throughout the whole purification and identification process, so that full technical replicates were obtained and enabled the exclusion of residual unspecific contaminations in the TAP outputs.

Construction and Evaluation of the PPI Network of the Proteins Involved in the Hypusine Modification System—After MS/MS analysis, 550 proteins were identified in all analyzed MS/MS samples. By application of both the bead proteome and replication filters, we were able to identify 248 proteins that potentially interact with the four HMS proteins. The filtered lists of proteins identified in this study are provided in supplemental Table S1, together with the list of proteins flagged as bead proteome. Furthermore, information about identification of proteins by mass spectrometry is provided in supplemental Table S2–S4. Revision of the bead proteome dataset revealed that it contained eIF-5A1 as one of the nonspecifically purified proteins. As this protein was used as a bait protein, and as its interaction to the other bait proteins is well-documented within the literature, we decided to omit

removing eIF-5A1 from the remaining datasets upon application of the bead proteome filter. As the main focus of this study was to identify unknown PPI of the HMS, the inclusion or exclusion of eIF-5A1 in the data set was of no practical consequence.

To annotate the biological relevance of the newly identified PPI, we next analyzed the proteins in several ways: first, we constructed an interconnected network from our list of specifically interacting proteins as described in "experimental procedures" (Fig. 2*A*). Nodes with red borders represent proteins that were identified previously, but not in this study. These proteins were excluded from further analyses. Notably, database searches revealed only 35 known mammalian interaction partners, 10 of which were also identified in our TAP outputs (Fig. 2*B*). Thus, this study reports approximately seven times the number of proteins to be involved in the HMS, compared with formerly available studies. Between eIF-5A1 and eIF-5A2, a significant overlap of 72 proteins exists that represents 33.3% of the eIF-5A1 and 82.8% of the eIF-5A2 dataset. Moreover, 138 (55.2% of total) proteins were uniquely detected with eIF-5A1 (supplemental Fig. S3). A significant number of proteins nevertheless appeared to display isoform-specific interactions, supporting the idea of specialized functions for these proteins.

We next concentrated our analysis on enriched functional clusters contained in the network (Figs. 3*A* to 3*E*). Cluster analysis of a network can indicate functional modules of protein complexes that were copurified with the bait protein (53), hence we applied cluster analysis to our entire HMS network. This approach revealed five significantly interconnected functional clusters, the largest one consisting of 18 ribosomal proteins of the large subunit, three proteins of the small ribosomal subunit, and the translation initiation factors eIF-2α (eIF2s1, Q6ZWX6), eIF3a (P23116), and eIF3b (Q8JZQ9), and eIF-4B (Q8BGD9), and eIF-5B (Q05D44), totaling 26 proteins with a p value of 1.38×10^{-9} (Fig. 3*A*). Another cluster included 10 nuclear proteins that are mainly active in RNA processing and transport ($p = 8.65 \times 10^{-5}$), namely U2af2 (P26369), SF3b130 (Q921M3), ASF/SF2 (Q6PDM2), serine/arginine-rich splicing factor 7 (Q8BL97), hnRNP A2/B1 (O88569), -D0 (Q60668), -U (Q8VEK3), and -X (α-CP2, Q61990), Ptbp1 (P17225), and nuclear RNA export factor 1 (Q99JX7) (Fig. 3*B*). Six members of the T-complex chaperonin family (TCP-1-γ (P80318), -δ (P80315), -ϵ (P80316), -η (P80313), and -θ (P42932), as well as Cct6a (P80317)), comprised a third cluster ($p = 0.002$) (Fig. 3*C*). The three RNA-binding proteins nucleolin, NPM (Q61937) and tRNA (cytosine-5)-methyltransferase NSUN2 (Q1HFZ0), as well as four proteins active in mitosis and cell cycle control (Ckap5 (A2AGT5), RCC2 (Q8BK67), and kinesin-like proteins KIF2A (P28740) and KIF2C (Q9QWT9)) are contained in the remaining two clusters ($p = 0.029$ and $p = 0.039$, respectively) (Figs. 3*D* and 3*E*).
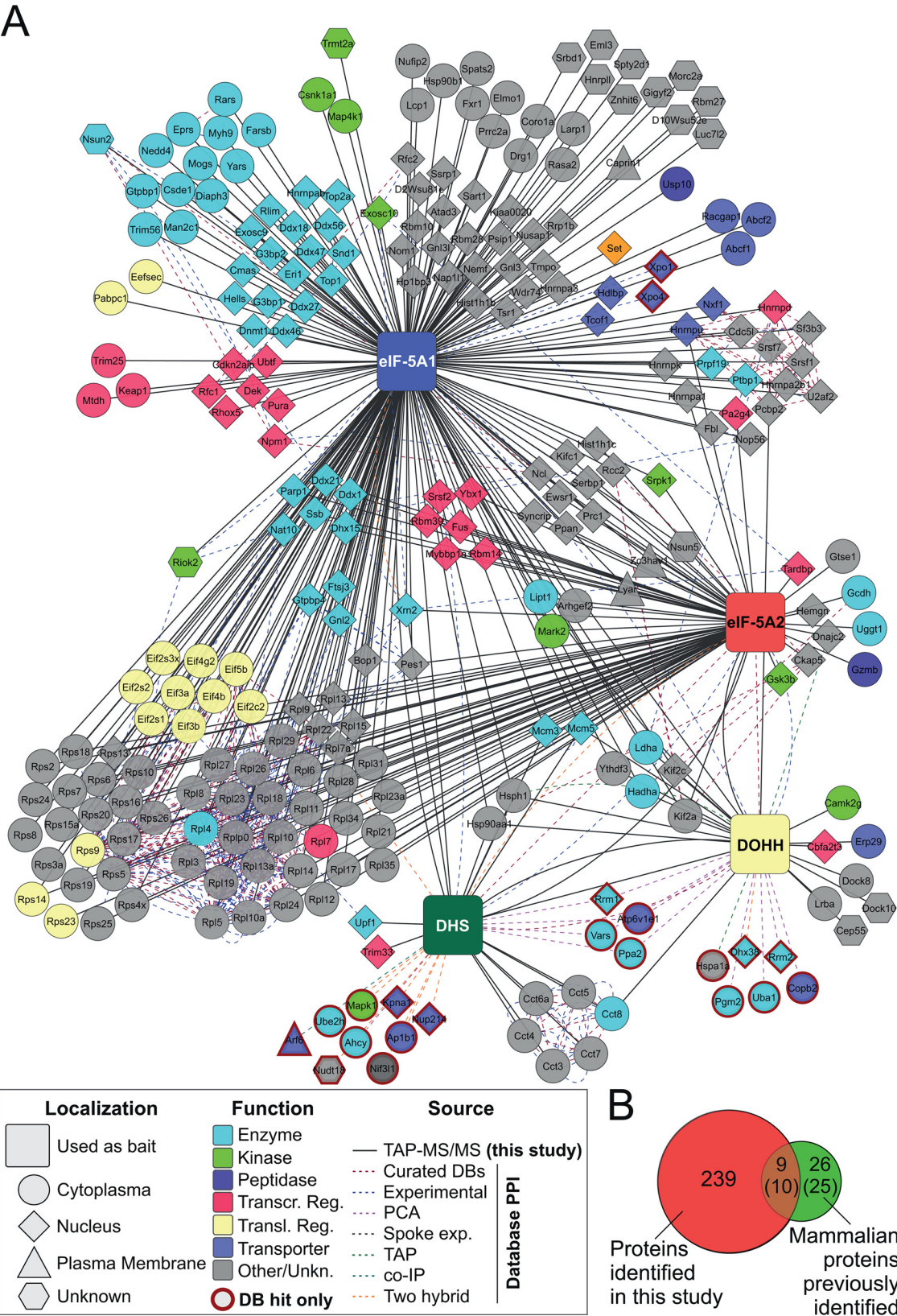
FIG. 2. **A comprehensive protein-protein interaction network of the hypusine modification system.** *A*, A spoke network of the four sets of identified proteins (own data, solid edges) was interconnected by querying the STRING and IntAct databases with all identified proteins for experimentally determined interactions and those listed in manually curated databases (previously existing external data, dashed edges). Main
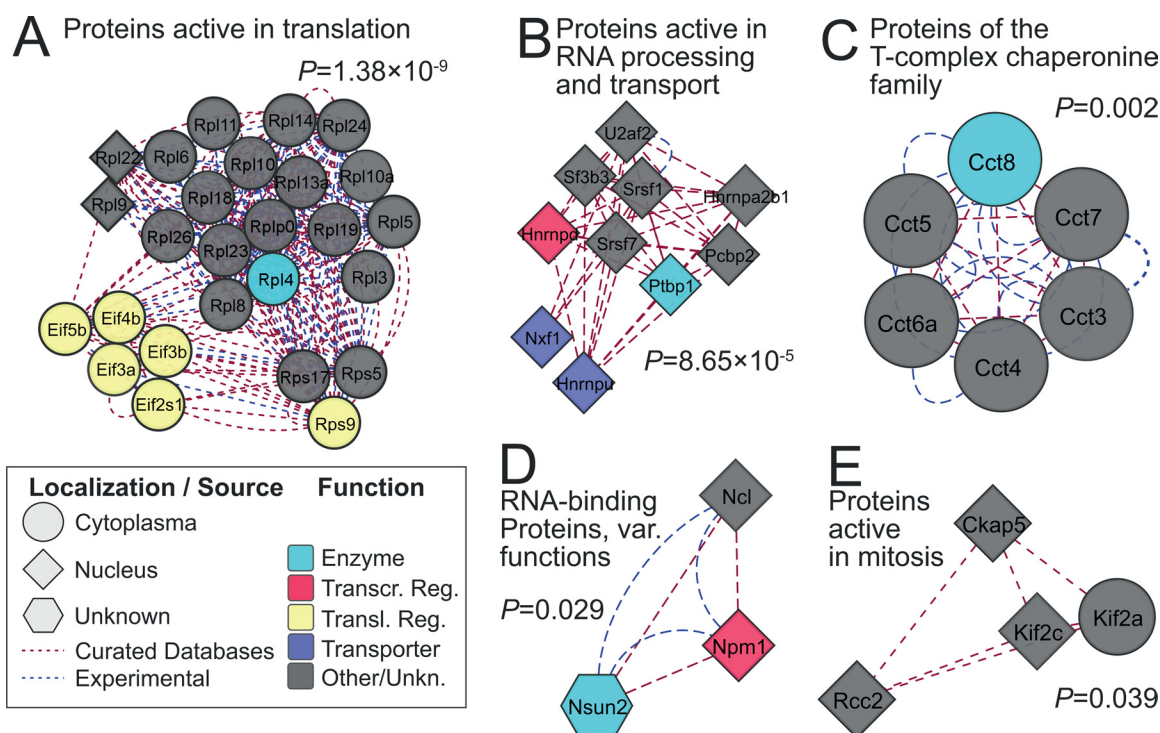
Fig. 3. **Identification of protein-protein interaction (PPI) clusters of the hypusine modification network.** *A–E*, The network shown in Fig. 2*A* was analyzed for significant PPI clusters via the ClusterONE Cytoscape plug-in. All clusters with $p < 0.05$ were extracted from the network and analyzed for common key protein functions. See legend for clarification of node and edge color and shape code.

We further compared our PPI network with a network built from data of high-throughput experiments in yeast, accessible via the IntAct (41) and STRING (40) databases (supplemental Fig. S4*A*). Of 115 interacting proteins that we were able to extract from these databases, we only processed 68 that we could assign to mammalian orthologs via the OMA browser (45). Twenty-six (38.2%) of these proteins' orthologs were also included in our data set, three of which were removed from our interaction network because of appearance in the bead proteome (supplemental Fig. S4*B*). Interaction enrichment of the intersecting yeast and mammalian protein sets via STRING and a direct comparison of both resulting networks showed that especially the interactions between eIF-5A and the ribosomal complex display high evolutionary conservation.

Gene ontology (GO) analysis reveals highly significant enrichment of interacting proteins implicated in translation and RNA metabolism.

To obtain a comprehensive view of the mammalian HMS interactome, we next asked whether specific molecular functions or biological processes were enriched in our sets of

identified proteins (supplemental Table S1). The gene ontology (GO) categories that were identified as significantly enriched in our datasets using the PANTHER (43, 44) database are shown in supplemental Fig. S5. In the top category "biological process," the most significantly enriched categories were "(protein) metabolic process" (which contains "translation"), as well as "cellular process" (and therein "cell cycle" and "cell communication"). The second dominant category in "metabolic process" was "nucleic acid metabolic process" (itself containing "RNA metabolic process"). The GO analysis for "molecular function" showed "catalytic activity" and "binding" as most enriched categories. Therein, the terms "helicase activity," "ligase activity," "transferase activity," "hydrolase activity," and "RNA splicing factor activity," as well as "nucleic acid binding" and "protein binding," respectively, were returned as the most enriched subcategories. Collectively, these findings further support the commonly proposed roles for eIF-5A in protein translation, RNA metabolism and transport, as well as cell cycle regulation. However, proteins annotated to other ontologies are also enriched in the four datasets to various degrees according to the GO report, hint-

localizations (node shape) and functions (node color) of proteins were queried from Ingenuity Pathway Analysis. See legend for clarification of node and edge color and shape code. Proteins represented by red-bordered nodes were not identified in this study but have been reported as putative interaction partners by other studies. *B*, Comparison of the numbers of proteins identified in this study and those obtained from online databases. Values in parentheses include proteins that were removed with the "bead proteome" filter. Note that our method has identified 239 new proteins as putative interaction partners of HMS members.

ing at possible additional unidentified cell biological roles of the HMS.

Validation of Novel Interaction Partners Using a Protein Fragment Complementation Assay (PCA)—As an initial validation method, we used a protein fragment complementation assay (PCA) employing split-YFP fusion proteins (31) (Fig. 4A). We first tested the applicability of this assay to our bait proteins, using the previously reported homodimerization of eIF-5A as well as its interaction with both DHS and DOHH as positive control experiments. As shown in Figs. 4B and 4C, both DHS- and DOHH-YFP$_2$ fusions elicited significant enhancement of fluorescence over background levels in combination with the eIF-5A1-YFP$_1$ fusion. Similar fluorescent enhancement was also observed when eIF-5A1-YFP$_1$ was tested with YFP$_2$ fusions of eIF-5A1. In contrast, no enhancement over background was observed when MCFD2-YFP$_1$ was tested with the respective YFP$_2$ fusions as a negative control. However, MCFD2-YFP$_1$ combined with ERGIC-53-YFP$_2$, a known interaction partner of this protein (31), showed a positive signal comparable to those of the eIF-5A combinations (Fig. 4B). These effects could also be confirmed by fluorescence microscopy (Fig. 4C). Interestingly, the combination of DHS and eIF-5A fusion proteins resulted in the occurrence of small speckles of high and only little diffuse fluorescence activity (Fig. 4C, *right* panel). We concluded that this YFP-based PCA approach can specifically detect interactions between components of the HMS and its protein interaction partners.

To assess the reliability of our bioreactor-TAP-MS/MS results, a sample set of seven proteins occupying key functions or central positions in the general interaction network, namely EF-2 (Q60875), ATP-dependent RNA helicase, PAI-RBP1 (Q9CY58), TDP-43 (Q921F2), LDH-A (P06151), DNA replication licensing factor MCM5 (P49718), and NPM (Q61937), as well as DDX3X (Q62167) as a member of the "bead proteome" filter, were tested in experiments aimed at validating these proteins' network connections by reciprocal TAP and in viable cells using the PCA (Figs. 4D–4G). eIF-5A1 displayed significant close-range interactions with EF-2, PAI-RBP1, TDP-43, LDH-A and NPM (Fig. 4D). Interactions with PAI-RBP1, TDP-43, and NPM could also be confirmed for eIF-5A2. However, the putative interaction between EF-2 and eIF-5A2 was less pronounced and did not reach statistical significance (Fig. 4E). DHS and DOHH both showed significant interaction with LDH-A, and DOHH also interacted with pyruvate kinase isozymes M1/M2 (P52480), which was uniquely identified in one of the DOHH (SG) technical replicates (Figs. 4F and 4G). For eIF-5A1, 5 of 7 tested proteins could be confirmed, all of which were identified in bioreactor-TAP-MS/MS using eIF-5A1 as bait. The remaining two proteins (MCM5 and DDX3X) were identified in all HMS sets and likely represent proteins that belong into the bead proteome category. In fact, DDX3X was also identified in MS/MS samples from eGFP (SG) TAP experiments and thus removed from the adjusted dataset

upon application of the bead proteome filter. For the PCA combinations involving the other HMS proteins, not all of the tested proteins were also found in the respective bioreactor-TAP-MS/MS sets. Because most tested proteins that were also identified as interaction partners in the bioreactor-TAP-MS/MS did interact with the respective baits, these findings confirm the general validity of our TAP-MS/MS data.

The eIF-5A Protein Displays Hypusine-independent Interactions with Ribosomal Proteins Rpl10a and Rps5—Consistent with eIF-5A's proposed function in translation, we identified numerous ribosomal proteins in our purification protocol. A recent report described the crystal structure of the prokaryotic ortholog of eIF-5A, EF-P, bound to the prokaryotic 70S ribosome. This study revealed that EF-P's interaction with the 70S ribosome occurs directly adjacent to the ribosomal proteins Rps7p and Rpl1p (54). As both eukaryotic orthologs of these proteins, 40S ribosomal protein S5 (Rps5, P97461) and 60S ribosomal protein L10a (Rpl10a, P53026), also appeared in the TAP-MS/MS results (supplemental Table S1), we chose to analyze their interactions with eIF-5A in greater detail. As expected, both eIF-5A isoforms showed significant interaction with both ribosomal proteins in the PCA (Figs. 5B, 5D, 5F, and 5H). Fluorescence microscopy images showed the characteristic pattern of ribosomal proteins, with high signal intensity in nucleoli and a lower diffuse fluorescence emitted from the cytoplasm and nucleus (Figs. 5A, 5C, 5E, and 5G). Because nonhypusinated eIF-5A is inactive in protein translation and/or initiation (55, 56), we expected the interaction to involve the N-terminal region of eIF-5A, as it harbors the Lys$_{50}$ residue that is eventually modified to hypusine. Although both eIF-5A$_{1-83}$ isoforms showed a trend of elevated fluorescence intensity, only eIF-5A1$_{1-83}$/Rps5 and eIF-5A2$_{1-83}$/Rpl10a reach statistical significance (Figs. 5F and 5D, respectively). However, none of the four combinations involving eIF-5A$_{84-154}$ showed significant interactions, highlighting the N terminus as the primary site for ribosomal interaction of eIF-5A. Interestingly, the association of eIF-5A with these proteins could not be significantly reduced by the introduction of point mutants that render eIF-5A hypusine-deficient, indicating that the interaction of eIF-5A1 and eIF-5A2 with these components of the ribosomal complex occurs in a hypusine-independent fashion. Reciprocal TAP experiments using Rps5 and Rpl10a as bait proteins, followed by Western blot detection of eIF-5A1, showed a positive signal only in case of Rps5, but not with Rpl10a (Fig. 5I).

NPM and TDP-43 also Show Interactions with eIF-5A—Our interaction network revealed the previously unknown interaction of eIF-5A with NPM and TDP-43, two proteins that presumably have no general role in mRNA translation. We further analyzed these particular proteins in order to gain more insight into potential eIF-5A functions outside of translation (Fig. 6). Notably, TDP-43 displayed the strongest interactions with eIF-5A both in PCA and Western blot analysis of reciprocal TAP experiments (Figs. 4D and 4E, Figs. 6B, 6D, and 6I).
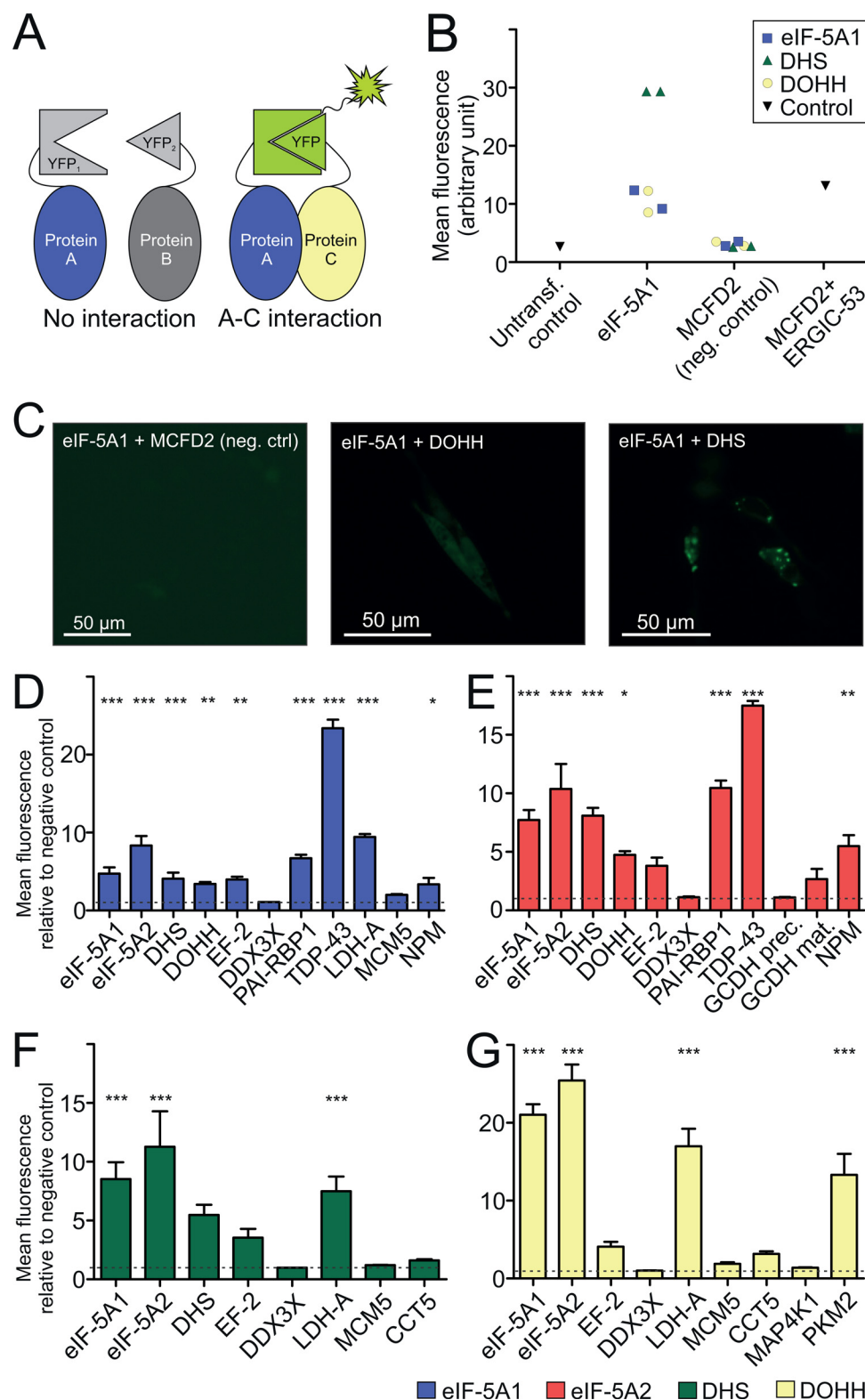
FIG. 4. **Establishment of a protein fragment complementation assay (PCA) assay to validate newly identified PPI.** *A*, Mechanism of the split-YFP PCA assay: upon interaction of proteins A and C, the YFP fragments can fold into YFP's native state, leading to fluorescence activity (*B*) Flow cytometric evaluation of previously known PPI and negative controls involving eIF-5A1- and MCFD2-YFP$_1$. Corresponding YFP$_2$-coupled protein is indicated by shape. MCFD2-YFP$_1$ and ERGIC-53-YFP$_2$ are known to interact (31) and show MCFD2-YFP$_1$ is expressed and functional, confirming its applicability as negative control. Values represent mean fluorescence of viable cotransfected cells. *C*, Representative

TDP-43 is a DNA- and RNA-binding protein that has previously been implicated in the regulation of transcription and splicing, and is linked to neurodegenerative disease (reviewed in (57)). By analyzing eIF-5A mutants, we found that an interaction of eIF-5A1 to TDP-43 was detectable using the N-terminal domain of eIF-5A1, but not its C-terminal domain (Fig. 6B). As the eIF-5A1$_{1-83}$/TDP-43 signal reaches only about 40% of the wild type combination, the C-terminal domain seems to also be involved in some aspect of the interaction, without specifically binding to TDP-43 itself. Additionally, both the eIF-5A1$_{K50R}$ and the eIF-5A1$_{G52A}$ mutants showed significantly diminished interaction with TDP-43 compared with the wild type form, consistent with a significant dependence on hypusine formation for this interaction (Fig. 6B). For the different forms of eIF-5A2, the PCA showed less pronounced differences in TDP-43 interaction (Fig. 6D). Thus, our data validate NPM and TDP-43 as additional direct or indirect binding partners of eIF-5A that, in case of TDP-43, interact in a hypusine-dependent fashion.

The eIF-5A and DHS Proteins Show Partial Colocalization to Cytoplasmic Multivesicular Bodies (MVBs) in PCA Experiments—As shown in Fig. 4C, we reproducibly observed very low diffuse cytoplasmic fluorescence and speckles of high YFP signal intensities in PCA experiments conducted to determine the interaction of both isoforms of eIF-5A with DHS (Fig. 7A). We were unable to elicit a similar effect with any other binding partner of eIF-5A or DHS. Furthermore, the overexpression of eGFP-tagged fusion proteins of either eIF-5A or DHS alone resulted in the expected, diffuse cytoplasmatic fluorescence signal, and no speckles of high fluorescence activity were observed (supplemental Fig. S6). To exclude the possibility that these speckles represent unspecific protein aggregation, experiments were conducted with various eIF-5A mutants and DHS in combination with GC7 (N$_1$-guanyl-1,7-diaminoheptane), a small molecular weight DHS-inhibitor that impedes hypusine formation (58). In contrast to the mutant forms eIF-5A$_{G52A}$ and eIF-5A$_{84-154}$, wild type eIF-5A1, eIF-5A1$_{1-83}$, and eIF-5A1$_{K50R}$ evoked the formation of YFP spot-like signals. Moreover, inhibition of DHS by 20 μM of GC7 appeared to inhibit this specific cytoplasmic localization, strongly suggesting that DHS enzymatic activity is required for this localization pattern (Fig. 7A). We then tested whether these fluorescent speckles occurred because of the localization of eIF-5A/DHS to specific cytoplasmic organelles. Some organelles or organelle-related mechanisms have been previously reported to be associated with eIF-5A activity, including the endoplasmatic reticulum (ER) (59), autophagosomes (60), processing bodies (PB) (55), and stress

granules (SG) (61). We therefore performed various colocalization studies, analyzing the aforementioned compartments as well as endosomal sorting complex required for transport I (ESCRT-I) complex subunit TSG101 (TSG101). This protein is located at late endosomal multivesicular bodies (MVB), primarily orchestrating intracellular protein sorting and trafficking (62). For this we generated various fluorescent fusion marker proteins and cotransfected these respective expression vectors together with our eIF-5A/DHS PCA constructs. In addition, the desired localization patterns of autophagosome marker protein autophagy-related protein LC3 (LC3) and SG-marker TIA-1 were induced by chloroquine or puromycin treatment, respectively. The fluorescence microscopy analyses revealed that the majority of these marker proteins did not significantly colocalize with eIF-5A/DHS (supplemental Fig. S7A). In contrast, signals that appeared in the respective channel of mRFP-TSG101 or Cer2-TSG101 cotransfected cells partially overlapped with the eIF-5A/DHS speckles in the YFP channel (Fig. 7B). We then performed fluorescence-based immunolabeling of a second endosomal marker, early endosome antigen 1 (EEA1), a protein located primarily in the membranes of early endosomes with a role in endosomal trafficking. As shown in Fig. 7C, speckles of eIF-5A1/DHS PCA cotransfected cells colocalized with EEA1. On the other hand, the ER-marker calreticulin did not show a similar significant colocalization to eIF-5A/DHS within the same experimental setting (supplemental Fig. S7B). These observations suggest that the eIF-5A/DHS interaction may take place either in association with or in close proximity to components of the endosomal pathway.
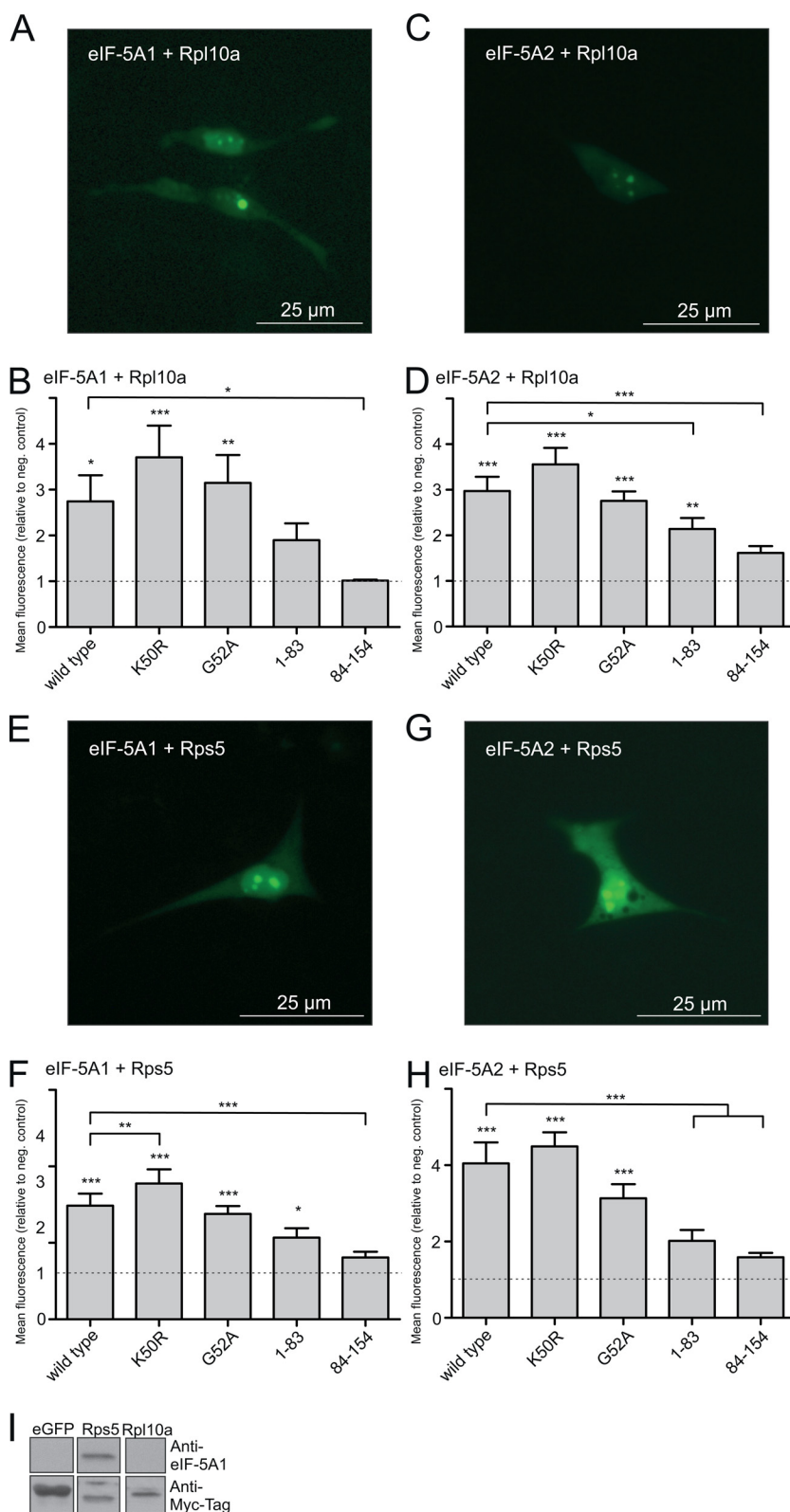
DISCUSSION

Hypusine is a unique post-translational modification that mediates important cellular functions and has been demonstrated to be involved in the pathogenesis and development of cancer and other highly prevalent diseases like diabetes and AIDS (reviewed in (63–65)). As such, it potentially represents a unique target for the development of novel therapeutic approaches in these conditions (reviewed in (66)). To elucidate the role of the unique hypusine-containing eIF-5A protein in cell biology and pathology in more detail, we have combined a TAP-MS/MS approach with the production of high amounts of cellular input material in a bioreactor, ensuring reproducible culture conditions, and applied it to all four proteins of the HMS.

In the resulting dataset, factors related to protein synthesis represent the biggest subgroup of the 231 identified proteins copurified with both eIF-5A isoforms (52.4% and 70.2% for

---

microscopic pictures of a control combination (eIF-5A2 + MCFD2) and a known interaction (eIF-5A2 + DOHH). The elevated background of the control originates from prolonged exposure. *D–G*, Flow cytometric quantification of PCA experiments with combinations of known and newly identified putative interaction partners. Bars represent mean fluorescence of two independent runs of duplicates ($n = 4$) normalized to negative control experiments (gray dashed lines). Error bars represent standard error of the mean (S.E.). Asterisks (*) represent statistically significant variation from the respective negative control (* $p < 0.05$; ** $p < 0.01$; *** $p < 0.001$).
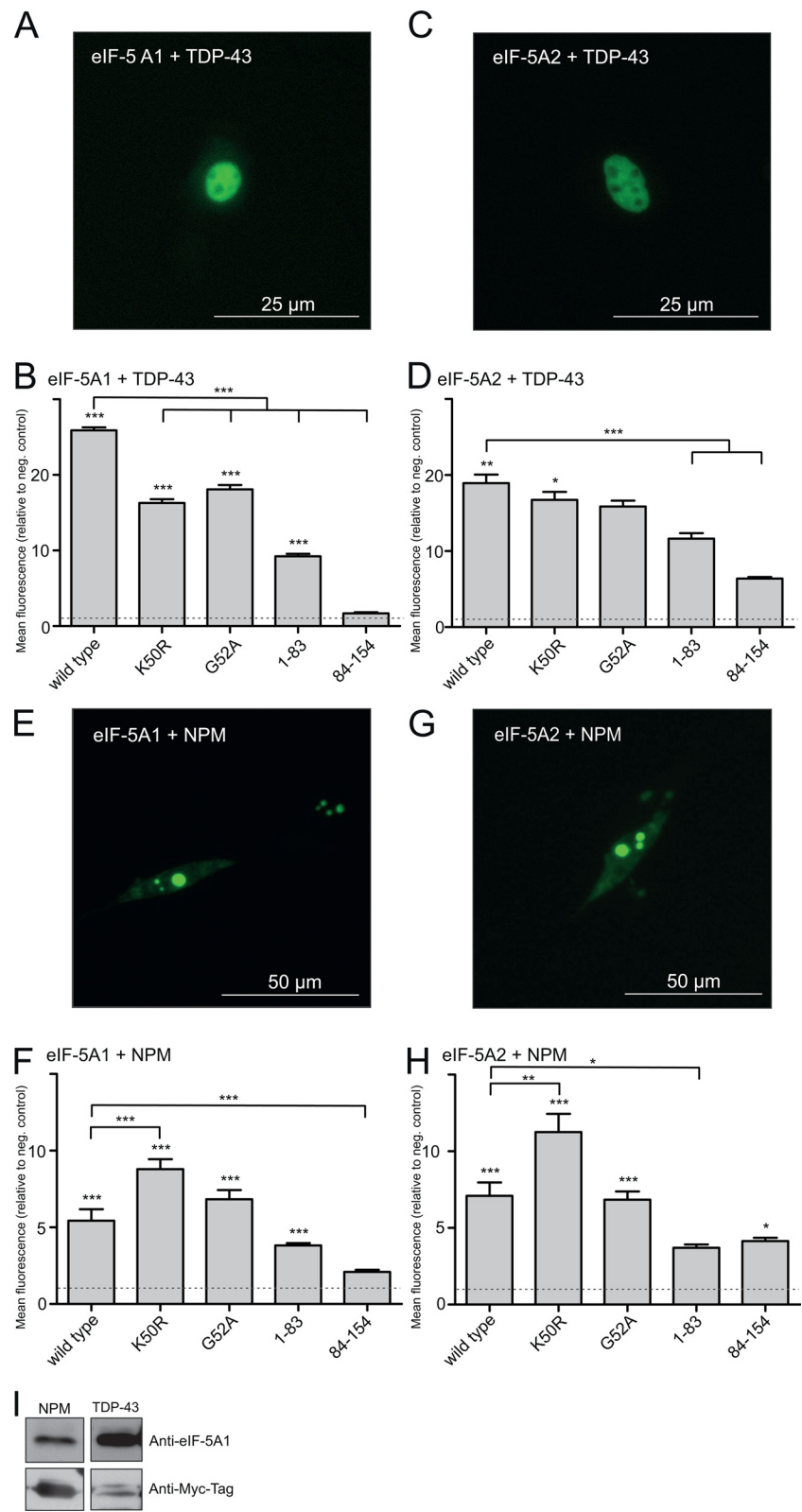
Fig. 5. **Validation and further evaluation of putative eIF-5A interactions with RPS5 and RPL10a.** (*A*, *C*, *E*, and *G*) Fluorescence microscopy images of representative YFP-positive cells of PCA experiments as indicated on panels. (*B*, *D*, *F*, and *H*) Flow cytometric quantification of PCA experiments as indicated on panels. Bars represent mean fluorescent values of two independent runs of duplicates ($n = 4$) normalized to negative control experiments (*dashed lines*). Error bars represent S.E. Asterisks (*) represent statistically significant variation from the respective control or the wild type combination (* $p < 0.05$; ** $p < 0.01$; *** $p < 0.001$). *I*, Western blots of TAP outputs from reciprocal pull-down experiments employing newly identified putative eIF-5A interaction partners as bait proteins and eGFP (SG) as negative control. Anti-Myc-tag detects bait proteins via the TAP-tag. All outputs were processed on the same gel/membrane, all shown bands originate from the same exposure.

eIF-5A1 and eIF-5A2, respectively), as defined by GO categories. As expected, the most significant cluster that we identified in our hypusine network was exclusively composed of proteins related to ribosomal function. However, we were also able to identify a large number of additional proteins that have been reported to elicit completely different function and might

FIG. 6. **Validation and further evaluation of putative eIF-5A interactions with TDP-43 and NPM.** (*A*, *C*, *E*, and *G*) Fluorescence microscopy images of representative YFP-positive cells of PCA experiments as indicated on panels. (*B*, *D*, *F*, and *H*) Flow cytometric quantification of PCA experiments as indicated on panels. Bars represent mean fluorescent values of two independent runs of duplicates ($n = 4$) normalized to negative control experiments (*dashed lines*). Error bars represent S.E. Asterisks (*) represent statistically significant variation from the respective control or the wild type combination (* $p < 0.05$; ** $p < 0.01$; *** $p < 0.001$). *I*, Western blots of TAP outputs from reciprocal pull-down experiments employing newly identified putative eIF-5A interaction partners as bait proteins. Anti-Myc-tag detects bait proteins via the TAP-tag. All outputs were processed on the same gel/membrane, all shown bands originate from the same exposure.

help to shed light on the mechanisms that underlie the various eIF-5A activities. The previously proposed roles of eIF-5A in specific transport of mRNA, mRNA maturation, and mRNA stability in mammals (24, 67–69), coincide with the finding that a majority of the identified proteins (69.0% and 72.7%) in the eIF-5A datasets are classified as RNA-binding. This find-
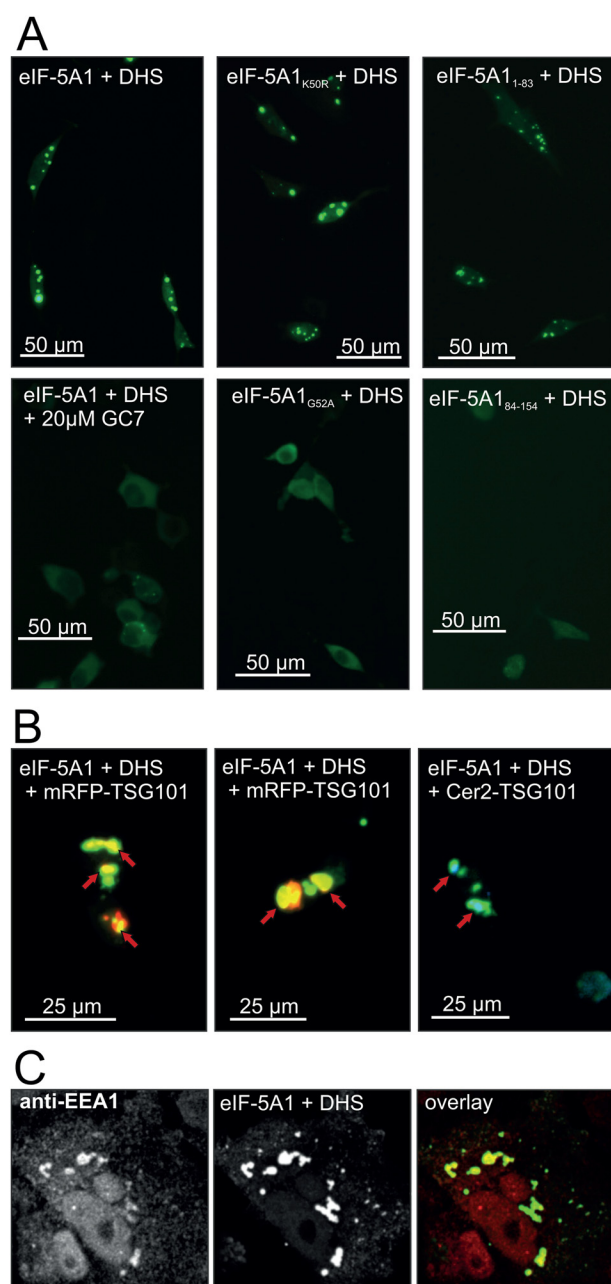
A

| eIF-5A1 + DHS | eIF-5A1$_{K50R}$ + DHS | eIF-5A1$_{1-83}$ + DHS |
| eIF-5A1 + DHS + 20μM GC7 | eIF-5A1$_{G52A}$ + DHS | eIF-5A1$_{84-154}$ + DHS |

B

| eIF-5A1 + DHS + mRFP-TSG101 | eIF-5A1 + DHS + mRFP-TSG101 | eIF-5A1 + DHS + Cer2-TSG101 |

C

| anti-EEA1 | eIF-5A1 + DHS | overlay |

FIG. 7. **Specificity and subcellular localization of observed eIF-5A1/DHS-complexes.** Fluorescence microscopy images showing representative YFP-positive cells from PCA experiments as indicated on the panels. Green channel, reconstituted YFP; red channel, mRFP or Alexa633 (immunolabeling experiments); blue channel, Cer2. *A*, Wild type eIF-5A1, the eIF-5A1$_{K50R}$ mutant and the N-terminal domain of eIF-5A1 show YFP speckles upon binding of DHS in PCA experiments. The eIF-5A1$_{G52A}$ mutant, the C-terminal domain of eIF-5A1 and addition of 20 μM GC7 disrupt this localization of eIF-5A1/DHS PCA complexes. *B*, A fusion protein from fluorescent proteins mRFP or Cer2, respectively, and TSG101 (member of the ESCRT-I protein family and marker for MVBs) showed significant colocalization with eIF-5A1/DHS PCA complexes. Most double-positive cells showed more speckles of eIF-5A1/DHS PCA complex localization than MVBs, but the majority of labeled MVBs colocalized to eIF-5A1/DHS PCA complexes. *C*, Immunolabeled EEA1 (marker for early endosomes)

ing is further supported by cluster analysis, which revealed two clusters in our network that are mostly comprised of RNA-binding proteins active in RNA transport, processing and translation. The final overrepresented subgroup of proteins in GO and cluster analysis has regulatory functions in the cell cycle. This finding is particularly intriguing, because it suggests that the effects of eIF-5A on control of cellular proliferation may involve direct communication with the cell cycle control machinery, rather than simply being a downstream consequence of effects on gene expression, and might help to further explain observed cellular growth phenotypes after HMS inhibition. Indeed, this finding is consistent with recent studies that report eIF-5A to be crucially involved in normal and aberrant proliferation control (70, 71).

The comparison of available data from high-throughput studies in yeast (available via the IntAct database) and the data set presented in this study shows remarkable differences, as all common orthologs of proteins binding to eIF-5A are related to protein translation and none of the identifiable yeast orthologs of the proteins with different functional relationships were also found in yeast-based studies. A possible hypothesis that provides an explanation for these observations is that, whereas the translational regulatory function mediated by ribosome interaction may be the original function of eIF-5A and is highly conserved in evolution, additional roles for eIF-5A in the biology of more complex multicellular organisms might have developed over time. The fulfillment of this broader spectrum of cell biological functions would then require a commensurate extension of the set of interaction partners. In support of this hypothesis, phenotypes of mutations in yeast and *D. melanogaster* DOHH orthologs (LIA1 and *nero*, respectively) show remarkable differences: whereas LIA1-activity depleted yeast cells elicit only a mild reduction of their growth rate (17), *Drosophila* develops negative and eventually fatal effects on organism viability, organ development and processes like cell growth, proliferation and autophagy (72).

The idea of diverged eIF-5A functions in multicellular organisms may also extend to the protein isoforms themselves. As our data also identify significant differences in PPI for both isoforms, it seems reasonable to hypothesize that, beyond shared ancestral and "add-on" functions, eIF-5A1 executes a universal set of functions in cells of most or all tissues, whereas eIF-5A2 has developed other, more tissue-specific functions, for example in embryonic development or the nervous system. It is possible that this specialization also entails isoform-specific roles of eIF-5A in dedifferentiation and mobilization of cancer cells. In possible support of this notion, up-regulation of eIF-5A2—but not eIF-5A1—expression has been detected in hepatocellular carcinoma and could be con-

also showed significant colocalization with eIF-5A1/DHS PCA complexes.

nected to metastasis thereof, and is a prognostic marker for clinical outcome of lung cancer patients (22). Of note, eIF-5A2 has also been implicated in development of ovarian cancer and therefore been considered as an oncogene (21). Intriguingly, we have identified cytoskeleton-associated protein 5, which is over-expressed in hepatomas and colonic tumors (73), as a selective interaction partner specifically of eIF-5A2 (Fig 2*A*, supplemental Table S1). The expression in testis and CNS, as well as a study screening for mutations of the gene encoding human eIF-5A2 (EIF5A2) in infertile men (74), also suggest a special role of eIF-5A2 in spermatogenesis and neuronal function. Other newly identified interactions with eIF-5A2 (but not eIF-5A1) are also compatible with this supposition: GSK-3β (Q9WV60), which is highly expressed in testis and involved in cell migration regulation (75), GCD (Q60759), which is connected to glutaric aciduria type 1 (76), and UGT1 (Q6P5E4), which is highly expressed in brain tissue, all interact selectively with eIF-5A2. TDP-43, which is connected to amyotrophic lateral sclerosis type 10 (77), has been identified in the eIF-5A2 dataset by bioreactor-TAP-MS/MS and was found to interact with both isoforms of eIF-5A during experimental validation. It is important to note that the identification of PPI that mediate cellular functions specific to certain tissues might be impossible in cells derived from other tissues. Thus, a screening for eIF-5A2 binding partners in a neuronal or male germ cell context would presumably result in a different, arguably larger set of putative interaction partners. However, it is noteworthy that half of the eIF-5A2-specific subset found in our screening in pro-B lymphocytes is composed of proteins that are reported to be highly expressed and to have specific functions in brain and testis biology and pathophysiology.

To our knowledge, this is the first time that DHS and DOHH have been selectively screened for unknown PPI partners. However, in contrast to eIF-5A, our data do not suggest a similar functional diversity for the enzymes DHS and DOHH. Compared with eIF-5A, we have identified only few putative interaction partners for DHS and DOHH, and both data sets share a significant overlap with the eIF-5A isoforms, suggesting direct interactions only with one of the respective bait proteins. Furthermore, we could not find significant sequence homology to the highly conserved hypusination site of eIF-5A in any of the proteins copurified with DHS and DOHH, suggesting that the mode of interaction in these cases would have to be different from that of eIF-5A. Taken together, this supports the hypothesis that the function of both of these enzymes is focused on the hypusine modification of eIF-5A. However, as both sets contain proteins that are active regulators of different phases in cell proliferation, including E3 ubiquitin-protein ligase TRIM33 (Q99PP7), CEP55 (Q8BT07), kinesin-like proteins KIF2A, and KIF2C as well as DNA replication licensing factors MCM3 (P25206) and MCM5, it is intriguing to speculate that DHS and DOHH activity, and thereby eIF-5A activation, might also be regulated in this context.

As discussed above, many of the proteins identified in this study provide important hints about postulated and potential unknown molecular and cellular functions of eIF-5A and the hypusine modification. Using hypusine-deficient and deletion mutants of eIF-5A in PCA and TAP experiments, we have determined the impact of hypusine on newly identified eIF-5A interactions. Of course, the absence of changes in PPI in hypusine-deficient eIF-5A does not necessarily imply that the respective function is unaffected. For instance, eIF-5A$_{K50R}$ shows specific interaction with DHS in PCA, even though eIF-5A$_{K50R}$ cannot be hypusinated and thus the interaction remains noneffective in functional terms.

In case of Rpl10a and Rps5, both eIF-5A$_{K50R}$ and eIF-5A$_{G52A}$ mutants did not show a reduction in signal intensity in the interaction with either Rps5 or Rpl10a. This is in contrast to data collected in yeast (78), which showed a remarkable decrease of copurified ribosomal proteins with hypusine deficient mutant compared with wild type eIF-5A. A possible interpretation for this difference is that the interaction of hypusine deficient mutant eIF-5A with the ribosome is not completely abolished, but has an increased dissociation constant that results in significant loss of copurification capacity. In our live-cell PCA, however, the strong association of split-YFP fragments after initial complementation might mask this effect of eIF-5A mutation. The binding of mutated eIF-5A might also be explained by the presence of endogenous eIF-5A and the occurrence of wild type/mutant eIF-5A dimerization with the wild type form bound to the ribosome. Another possibility is that we observe indirect interactions with the ribosome via actively translated mRNAs that bind eIF-5A in a hypusine-independent manner. This interaction might be lost over time during the purification process but would be detectable in PCA.

Nevertheless, the N-terminal deletion mutant showed a significant reduction of ribosomal interaction and the C-terminal, nonhypusinated domain showed no interaction with the analyzed ribosomal proteins, indicating that the interaction interface is in fact contained in the hypusine-containing domain of the protein. Moreover, the reciprocal TAP assay resulted in a difference of copurified eIF-5A1 with Rps5 and Rpl10a. Although copurification was detectable with Rps5, no eIF-5A1 signal was detectable using Rpl10a as bait. Although this observation might be effected by geometrically inhibiting the interaction because of the introduction of the sizeable TAP tag, it likely suggests a more robust association of eIF-5A to the 40S subunit of the ribosome.

One of the many RNA-binding proteins in the eIF-5A dataset is TDP-43, which exhibited the strongest eIF-5A interaction of all candidates included in our validation experiments. Interestingly, it has also been reported to be a primarily nuclear RNA-binding protein that regulates pre-mRNA splicing (57, 79). At this point we do not know if eIF-5A's interaction with TDP-43 is direct or mediated by RNA or other binding partners. However, the relative strength of the interaction as

compared with all other tested proteins together with our ability to detect it consistently in both our *in vivo* and *in vitro* interaction assays suggests it is more likely to be direct. An additional link to eIF-5A exists through the negative regulation of HIV-1 transcription (80), because eIF-5A1 is also a regulator of HIV-1 replication (25).

Taken together, the results of these validation assays confirmed the specificity of copurification in the bioreactor-TAP-MS/MS assay with eIF-5A and indicate that, whereas the interaction of these proteins selected for validation with eIF-5A is domain-specific, it does not seem to generally rely on the integrity of the hypusine modification. This finding is in conflict with several reports that showed an essential role of hypusination in eIF-5A function. We envisage three possible interpretations for these hypusine-independent interactions: (1) they are not important for eIF-5A function; (2) they are important for a hypusine-dependent eIF-5A function, even though they are not themselves hypusine-dependent; (3) the interactions are important for a hypothetical hypusine-independent function of eIF-5A. Differentiating between these scenarios will require further experiments to test the importance of these interactions in functional assays.

Finally, the finding that eIF-5A1 and DHS colocalize with components of the endosomal sorting complex machinery may indicate that hypusination of eIF-5A influences the intracellular trafficking and, thus, the localization of eIF-5A. Alternatively, its colocalization with ESCRT-I components may reflect a function that is unrelated to vesicular transport. Of note, evidence has been provided that particularly TSG101 plays a role in cell cycle control (see (81) and references therein). Similar activities have also been described for hypusine-modified eIF-5A (6, 10, 11). This might indicate that both, eIF-5A and TSG101 (or related factors), are components of the same pathway regulating the proliferation and survival of tumor cells.

In summary, we have presented the bioreactor-TAP-MS/MS procedure, making use of highly sensitive mass spectrometers and linking of the assay to high-quality cell production in a bioreactor, and produced evidence for its high reliability. Application to the HMS proteins generated new evidence for these proteins various functions. Moreover, our results are compatible with the idea of new 'add-on' functions of eIF-5A acquired during its evolutionary development, some of which may be isoform-specific and especially important for multicellular organisms. As with any screening approach, our results have generated a far greater number of hypotheses about hypusine dependent molecular and cellular functions than could possibly be addressed in the present study; these will be the subject of future studies. Indeed, for this very reason, we are confident that the ongoing search for molecular mechanisms that can comprehensively explain eIF-5A functions will benefit significantly from this rich resource.

REFERENCES

1. Lemmon, M. A., and Schlessinger, J. (2010) Cell signaling by receptor tyrosine kinases. *Cell* **141,** 1117–1134
2. Martin, C., and Zhang, Y. (2005) The diverse functions of histone lysine methylation. Nature reviews. *Mol. Cell Biol.* **6,** 838–849
3. Yang, X. J., and Seto, E. (2008) Lysine acetylation: codified crosstalk with other posttranslational modifications. *Mol. Cell* **31,** 449–461
4. Kitano, H. (2004) Biological robustness. Nature reviews. *Genetics* **5,** 826–837
5. Cooper, H. L., Park, M. H., and Folk, J. E. (1982) Posttranslational formation of hypusine in a single major protein occurs generally in growing cells and is associated with activation of lymphocyte growth. *Cell* **29,** 791–797
6. Park, M. H., Lee, Y. B., and Joe, Y. A. (1997) Hypusine is essential for eukaryotic cell proliferation. *Biol. Signals* **6,** 115–123
7. Templin, A. T., Maier, B., Nishiki, Y., Tersey, S. A., and Mirmira, R. G. (2011) Deoxyhypusine synthase haploinsufficiency attenuates acute cytokine signaling. *Cell Cycle* **10,** 1–7
8. Park, M. H., and Wolff, E. C. (1988) Cell-free synthesis of deoxyhypusine. Separation of protein substrate and enzyme and identification of 1,3-diaminopropane as a product of spermidine cleavage. *J. Biol. Chem.* **263,** 15264–15269
9. Abbruzzese, A., Park, M. H., and Folk, J. E. (1986) Deoxyhypusine hydroxylase from rat testis. Partial purification and characterization. *J. Biol. Chem.* **261,** 3085–3089
10. Hanauske-Abel, H. M., Park, M. H., Hanauske, A. R., Popowicz, A. M., Lalande, M., and Folk, J. E. (1994) Inhibition of the G1-S transition of the cell cycle by inhibitors of deoxyhypusine hydroxylation. *Biochim. Biophys. Acta* **1221,** 115–124
11. Park, M. H., Wolff, E. C., Lee, Y. B., and Folk, J. E. (1994) Antiproliferative effects of inhibitors of deoxyhypusine synthase. Inhibition of growth of Chinese hamster ovary cells by guanyl diamines. *J. Biol. Chem.* **269,** 27827–27832
12. Wolff, E. C., Kang, K. R., Kim, Y. S., and Park, M. H. (2007) Posttranslational synthesis of hypusine: evolutionary progression and specificity of the hypusine modification. *Amino Acids* **33,** 341–350
13. Henderson, A., and Hershey, J. W. (2011) Eukaryotic translation initiation factor (eIF) 5A stimulates protein synthesis in Saccharomyces cerevisiae. *Proc. Natl. Acad. Sci. U. S. A.* **108,** 6415–6419
14. Saini, P., Eyler, D. E., Green, R., and Dever, T. E. (2009) Hypusine-containing protein eIF5A promotes translation elongation. *Nature* **459,** 118–121
15. Lipowsky, G., Bischoff, F. R., Schwarzmaier, P., Kraft, R., Kostka, S., Hartmann, E., Kutay, U., and Görlich, D. (2000) Exportin 4: a mediator of a novel nuclear export pathway in higher eukaryotes. *EMBO J.* **19,** 4362–4371
16. Ruhl, M., Himmelspach, M., Bahr, G. M., Hammerschmid, F., Jaksche, H., Wolff, B., Aschauer, H., Farrington, G. K., Probst, T. H., and Bevec, D. (1993) Eukaryotic initiation factor 5A is a cellular target of the human immunodeficiency virus type 1 Rev activation domain mediating transactivation. *J. Cell Biol.* **123,** 1309–1320
17. Park, M. H. (2006) The post-translational synthesis of a polyamine-derived amino acid, hypusine, in the eukaryotic translation initiation factor 5A (eIF5A). *J. Biochem.* **139,** 161–169
18. Schnier, J., Schwelberger, H. G., Smit-McBride, Z., Kang, H. A., and Hershey, J. W. (1991) Translation initiation factor 5A and its hypusine modification are essential for cell viability in the yeast Saccharomyces cerevisiae. *Mol. Cell. Biol.* **11,** 3105–3114

19. Caraglia, M., Marra, M., Giuberti, G., D'Alessandro, A. M., Baldi, A., Tassone, P., Venuta, S., Tagliaferri, P., and Abbruzzese, A. (2003) The eukaryotic initiation factor 5A is involved in the regulation of proliferation and apoptosis induced by interferon- and EGF in human cancer cells. *J. Biochem.* **133,** 757–765

20. Clement, P. M., Hanauske-Abel, H. M., Wolff, E. C., Kleinman, H. K., and Park, M. H. (2002) The antifungal drug ciclopirox inhibits deoxyhypusine and proline hydroxylation, endothelial cell growth and angiogenesis in vitro. *Int. J. Cancer* **100,** 491–498

21. Guan, X. Y., Fung, J. M. W., Ma, N. F., Lau, S. H., Tai, L. S., Xie, D., Zhang, Y., Hu, L., Wu, Q. L., Fang, Y., and Sham, J. S. (2004) Oncogenic role of eIF-5A2 in the development of ovarian cancer. *Cancer Res.* **64,** 4197–4200

22. He, L. R., Zhao, H. Y., Li, B. K., Liu, Y. H., Liu, M. Z., Guan, X. Y., Bian, X. W., Zeng, Y. X., and Xie, D. (2011) Overexpression of eIF5A-2 is an adverse prognostic marker of survival in stage I non-small cell lung cancer patients. *Int. J. Cancer* **129,** 143–150

23. Balabanov, S., Gontarewicz, A., Ziegler, P., Hartmann, U., Kammer, W., Copland, M., Brassat, U., Priemer, M., Hauber, I., Wilhelm, T., Schwarz, G., Kanz, L., Bokemeyer, C., Hauber, J., Holyoake, T. L., Nordheim, A., and Brümmendorf, T. H. (2007) Hypusination of eukaryotic initiation factor 5A (eIF5A): a novel therapeutic target in BCR-ABL-positive leukemias identified by a proteomics approach. *Blood* **109,** 1701–1711

24. Maier, B., Ogihara, T., Trace, A. P., Tersey, S. A., Robbins, R. D., Chakrabarti, S. K., Nunemaker, C. S., Stull, N. D., Taylor, C. A., Thompson, J. E., Dondero, R. S., Lewis, E. C., Dinarello, C. A., Nadler, J. L., and Mirmira, R. G. (2010) The unique hypusine modification of eIF5A promotes islet beta cell inflammation and dysfunction in mice. *J. Clin. Investig.* **120,** 2156–2170

25. Bevec, D., Jaksche, H., Oft, M., Wöhl, T., Himmelspach, M., Pacher, A., Schebesta, M., Koettnitz, K., Dobrovnik, M., Csonga, R., Lottspeich, F., and Hauber, J. (1996) Inhibition of HIV-1 replication in lymphocytes by mutants of the Rev cofactor eIF-5A. **271,** 1858–1860

26. Jenkins, Z. A., Hååg, P. G., and Johansson, H. E. (2001) Human eIF5A2 on chromosome 3q25-q27 is a phylogenetically conserved vertebrate variant of eukaryotic translation initiation factor 5A with tissue-specific expression. *Genomics* **71,** 101–109

27. Clement, P. M., Johansson, H. E., Wolff, E. C., and Park, M. H. (2006) Differential expression of eIF5A-1 and eIF5A-2 in human cancer cells. *FEBS J.* **273,** 1102–1114

28. Zender, L., Xue, W., Zuber, J., Semighini, C. P., Krasnitz, A., Ma, B., Zender, P., Kubicka, S., Luk, J. M., Schirmacher, P., McCombie, W. R., Wigler, M., Hicks, J., Hannon, G. J., Powers, S., and Lowe, S. W. (2008) An oncogenomics-based in vivo RNAi screen identifies tumor suppressors in liver cancer. *Cell* **135,** 852–864

29. Tang, D. J., Dong, S. S., Ma, N. F., Xie, D., Chen, L., Fu, L., Lau, S. H., Li, Y., Li, Y., and Guan, X. Y. (2010) Overexpression of eukaryotic initiation factor 5A2 enhances cell motility and promotes tumor metastasis in hepatocellular carcinoma. *Hepatology* **51,** 1255–1263

30. Bürckstümmer, T., Bennett, K. L., Preradovic, A., Schütze, G., Hantschel, O., Superti-Furga, G., and Bauch, A. (2006) An efficient tandem affinity purification procedure for interaction proteomics in mammalian cells. *Nat. Methods* **3,** 1013–1019

31. Nyfeler, B., Michnick, S. W., and Hauri, H. P. (2005) Capturing protein interactions in the secretory pathway of living cells. *Proc. Natl. Acad. Sci. U. S. A.* **102,** 6350–6355

32. Kimura, S., Noda, T., and Yoshimori, T. (2007) Dissection of the autophagosome maturation process by a novel reporter protein, tandem fluorescent-tagged LC3. *Autophagy* **3,** 452–460

33. Campbell, R. E., Tour, O., Palmer, A. E., Steinbach, P. A., Baird, G. S., Zacharias, D. A., and Tsien, R. Y. (2002) A monomeric red fluorescent protein. *Proc. Natl. Acad. Sci. U. S. A.* **99,** 7877–7882

34. Balabanov, S., Gontarewicz, A., Keller, G., Raddrizzani, L., Braig, M., Bosotti, R., Moll, J., Jost, E., Barett, C., Rohe, I., Bokemeyer, C., Holyoake, T. L., and Brümmendorf, T. H. (2011) Abcg2 overexpression represents a novel mechanism for acquired resistance to the multi-kinase inhibitor Danusertib in BCR-ABL-positive cells in vitro. *PLoS One* **6,** e19164

35. Schaletzky, M., Platas Barradas, O., Sievert, H., Balabanov, S., Zeng, A. P., and Portner, R. (2011) Cultivation strategies of a BA/F3 cell line for fundamental cell research. *BMC Proc.* **5,** P48

36. Wolff, E. C., Lee, S. B., and Park, M. H. (2011) Assay of deoxyhypusine

synthase activity. In: Pegg, A. E., and Casero, J., Robert A., eds. *Methods in molecular biology (Clifton, N.J.)*, pp. 195–205, Humana Press, Totowa, NJ

37. Dyshlovoy, S. A., Naeth, I., Venz, S., Preukschas, M., Sievert, H., Jacobsen, C., Shubina, L. K., Gesell Salazar, M., Scharf, C., Walther, R., Krepstakies, M., Priyadarshini, M., Hauber, J., Fedorov, S. N., Bokemeyer, C., Stonik, V. A., Balabanov, S., and Honecker, F. (2012) Proteomic profiling of germ cell cancer cells treated with aaptamine, a marine alkaloid with antiproliferative activity. *J. Proteome Res.* **11,** 2316–2330

38. Smoot, M. E., Ono, K., Ruscheinski, J., Wang, P. L., and Ideker, T. (2011) Cytoscape 2.8: new features for data integration and network visualization. *Bioinformatics* **27,** 431–432

39. Jain, E., Bairoch, A., Duvaud, S., Phan, I., Redaschi, N., Suzek, B. E., Martin, M. J., McGarvey, P., and Gasteiger, E. (2009) Infrastructure for the life sciences: design and implementation of the UniProt website. *BMC Bioinformatics* **10,** 136

40. Szklarczyk, D., Franceschini, A., Kuhn, M., Simonovic, M., Roth, A., Minguez, P., Doerks, T., Stark, M., Muller, J., Bork, P., Jensen, L. J., and von Mering, C. (2011) The STRING database in 2011: functional interaction networks of proteins, globally integrated and scored. *Nucleic Acids Res.* **39,** D561–D568

41. Aranda, B., Achuthan, P., Alam-Faruque, Y., Armean, I., Bridge, A., Derow, C., Feuermann, M., Ghanbarian, A. T., Kerrien, S., Khadake, J., Kerssemakers, J., Leroy, C., Menden, M., Michaut, M., Montecchi-Palazzi, L., Neuhauser, S. N., Orchard, S., Perreau, V., Roechert, B., van Eijk, K., and Hermjakob, H. (2010) The IntAct molecular interaction database in 2010. *Nucleic Acids Res.* **38,** D525–D531

42. Nepusz, T., Yu, H., and Paccanaro, A. (2012) Detecting overlapping protein complexes in protein-protein interaction networks. *Nat. Methods* **9,** 471–472

43. Mi, H., and Thomas, P. (2009) PANTHER pathway: an ontology-based pathway database coupled with data analysis tools. *Methods Mol. Biol.* **563,** 123–140

44. Thomas, P. D., Kejariwal, A., Campbell, M. J., Mi, H., Diemer, K., Guo, N., Ladunga, I., Ulitsky-Lazareva, B., Muruganujan, A., Rabkin, S., Vandergriff, J. A., and Doremieux, O. (2003) PANTHER: a browsable database of gene products organized by biological function, using curated protein family and subfamily classification. *Nucleic Acids Res.* **31,** 334–341

45. Schneider, A., Dessimoz, C., and Gonnet, G. H. (2007) OMA Browser–exploring orthologous relations across 352 complete genomes. *Bioinformatics* **23,** 2180–2182

46. Ummanni, R., Jost, E., Braig, M., Lohmann, F., Mundt, F., Barett, C., Schlomm, T., Sauter, G., Senff, T., Bokemeyer, C., Sultmann, H., Meyer-Schwesinger, C., Brümmendorf, T. H., and Balabanov, S. (2011) Ubiquitin carboxyl-terminal hydrolase 1 (UCHL1) is a potential tumour suppressor in prostate cancer and is frequently silenced by promoter methylation. *Mol. Cancer* **10,** 129

47. Ummanni, R., Mundt, F., Pospisil, H., Venz, S., Scharf, C., Barett, C., Falth, M., Kollermann, J., Walther, R., Schlomm, T., Sauter, G., Bokemeyer, C., Sultmann, H., Schuppert, A., Brümmendorf, T. H., and Balabanov, S. (2011) Identification of clinically relevant protein targets in prostate cancer with 2D-DIGE coupled mass spectrometry and systems biology network platform. *PLoS one* **6,** e16833

48. Cano, V. S., Jeon, G. A., Johansson, H. E., Henderson, C. A., Park, J. H., Valentini, S. R., Hershey, J. W., and Park, M. H. (2008) Mutational analyses of human eIF5A-1–identification of amino acid residues critical for eIF5A activity and hypusine modification. *FEBS J.* **275,** 44–58

49. Costa-Neto, C. M., Parreiras-E-Silva, L. T., Ruller, R., Oliveira, E. B., Miranda, A., Oliveira, L., and Ward, R. J. (2006) Molecular modeling of the human eukaryotic translation initiation factor 5A (eIF5A) based on spectroscopic and computational analyses. *Biochem. Biophys. Res. Commun.* **347,** 634–640

50. Park, M. H., Cooper, H. L., and Folk, J. E. (1981) Identification of hypusine, an unusual amino acid, in a protein from human lymphocytes and of spermidine as its biosynthetic precursor. *Proc. Natl. Acad. Sci. U. S. A.* **78,** 2869–2873

51. Glatter, T., Wepf, A., Aebersold, R., and Gstaiger, M. (2009) An integrated workflow for charting the human interaction proteome: insights into the PP2A system. *Mol. Syst. Biol.* **5,** 237

52. Trinkle-Mulcahy, L., Boulon, S., Lam, Y. W., Urcia, R., Boisvert, F.-M., Vandermoere, F., Morrice, N. A., Swift, S., Rothbauer, U., Leonhardt, H.,

and Lamond, A. (2008) Identifying specific protein interaction partners using quantitative mass spectrometry and bead proteomes. *J. Cell Biol.* **183,** 223–239

53. Wang, Z., and Zhang, J. (2007) In search of the biological significance of modular structures in protein networks. *PLoS Computational Biol.* **3,** e107

54. Blaha, G., Stanley, R. E., and Steitz, T. A. (2009) Formation of the first peptide bond: the structure of EF-P bound to the 70S ribosome. *Science* **325,** 966–970

55. Gregio, A. P., Cano, V. P., Avaca, J. S., Valentini, S. R., and Zanelli, C. F. (2009) eIF5A has a function in the elongation step of translation in yeast. *Biochem. Biophys. Res. Commun.* **380,** 785–790

56. Park, M. H., Wolff, E. C., Smit-McBride, Z., Hershey, J. W., and Folk, J. E. (1991) Comparison of the activities of variant forms of eIF-4D. The requirement for hypusine or deoxyhypusine. *J. Biol. Chem.* **266,** 7988–7994

57. Cook, C., Zhang, Y. J., Xu, Y. F., Dickson, D. W., and Petrucelli, L. (2008) TDP-43 in neurodegenerative disorders. *Expert Opin. Biol. Therapy* **8,** 969–978

58. Lee, C. H., and Park, M. H. (2000) Human deoxyhypusine synthase: interrelationship between binding of NAD and substrates. *Biochem. J. 352 Pt* **3,** 851–857

59. Frigieri, M. C., Thompson, G. M., Pandolfi, J. R., Zanelli, C. F., and Valentini, S. R. (2007) Use of a synthetic lethal screen to identify genes related to TIF51A in Saccharomyces cerevisiae. *Genetics Mol. Res.* **6,** 152–165

60. Patel, P. H., Costa-Mattioli, M., Schulze, K. L., and Bellen, H. J. (2009) The Drosophila deoxyhypusine hydroxylase homologue nero and its target eIF5A are required for cell growth and the regulation of autophagy. *J. Cell Biol.* **185,** 1181–1194

61. Li, C. H., Ohn, T., Ivanov, P., Tisdale, S., and Anderson, P. (2010) eIF5A promotes translation elongation, polysome disassembly and stress granule assembly. *PLoS One* **5,** e9942

62. Piper, R. C., and Katzmann, D. J. (2007) Biogenesis and function of multivesicular bodies. *Ann. Rev. Cell Develop. Biol.* **23,** 519–547

63. Caraglia, M., Marra, M., Giuberti, G., D'Alessandro, A. M., Budillon, A., Lentini, A., Beninati, S., and Abbruzzese, A. (2001) The role of eukaryotic initiation factor 5A in the control of cell proliferation and apoptosis. *Amino Acids* **20,** 91–104

64. Hauber, J. (2010) Revisiting an old acquaintance: role for eIF5A in diabetes. *J. Clin. Invest.* **120,** 1806–1808

65. Maier, B., Tersey, S. A., and Mirmira, R. G. (2010) Hypusine: a new target for therapeutic intervention in diabetic inflammation. *Discovery Med.* **10,** 18–23

66. Kaiser, A. (2012) Translational control of eIF5A in various diseases. *Amino Acids* **42,** 679–684

67. Hofmann, W., Reichart, B., Ewald, A., Müller, E., Schmitt, I., Stauber, R. H., Lottspeich, F., Jockusch, B. M., Scheer, U., Hauber, J., and Dabauvalle, M. C. (2001) Cofactor requirements for nuclear export of Rev response element (RRE)- and constitutive transport element (CTE)-containing retroviral RNAs. An unexpected role for actin. *J. Cell Biol.* **152,** 895–910

68. Rosorius, O., Reichart, B., Krätzer, F., Heger, P., Dabauvalle, M. C., and Hauber, J. (1999) Nuclear pore localization and nucleocytoplasmic transport of eIF-5A: evidence for direct interaction with the export receptor CRM1. *J. Cell Sci.* **112,** 2369–2380

69. Zuk, D., and Jacobson, A. (1998) A single amino acid substitution in yeast eIF-5A results in mRNA stabilization. *EMBO J.* **17,** 2914–2925

70. Cracchiolo, B. M., Heller, D. S., Clement, P. M., Wolff, E. C., Park, M. H., and Hanauske-Abel, H. M. (2004) Eukaryotic initiation factor 5A-1 (eIF5A-1) as a diagnostic marker for aberrant proliferation in intraepithelial neoplasia of the vulva. *Gynecol. Oncol.* **94,** 217–222

71. Ding, L., Gao, L. J., Gu, P. Q., Guo, S. Y., Cai, Y. Q., and Zhou, X. T. (2011) The role of eIF5A in epidermal growth factor-induced proliferation of corneal epithelial cell association with PI3-k/Akt activation. *Mol. Vision* **17,** 16–22

72. Patel, P. H., Costa-Mattioli, M., Schulze, K. L., and Bellen, H. J. (2009) The Drosophila deoxyhypusine hydroxylase homologue nero and its target eIF5A are required for cell growth and the regulation of autophagy. (Supplemental material). *J. Cell Biol.* **185,** 1181–1194

73. Charrasse, S., Mazel, M., Taviaux, S., Berta, P., Chow, T., and Larroque, C. (1995) Characterization of the cDNA and pattern of expression of a new gene over-expressed in human hepatomas and colonic tumors. *Eur. J. Biochem.* **234,** 406–413

74. Christensen, G. L., Ivanov, I. P., Atkins, J. F., Mielnik, A., Schlegel, P. N., and Carrell, D. T. (2005) Screening the SPO11 and EIF5A2 genes in a population of infertile men. *Fertility Sterility* **84,** 758–760

75. Kobayashi, T., Hino, S. I., Oue, N., Asahara, T., Zollo, M., Yasui, W., and Kikuchi, A. (2006) Glycogen synthase kinase 3 and h-prune regulate cell migration by modulating focal adhesions. *Mol. Cell. Biol.* **26,** 898–911

76. Keyser, B., Mühlhausen, C., Dickmanns, A., Christensen, E., Muschol, N., Ullrich, K., and Braulke, T. (2008) Disease-causing missense mutations affect enzymatic activity, stability and oligomerization of glutaryl-CoA dehydrogenase (GCDH). *Human Mol. Genetics* **17,** 3854–3863

77. Sreedharan, J., Blair, I. P., Tripathi, V. B., Hu, X., Vance, C., Rogelj, B., Ackerley, S., Durnall, J. C., Williams, K. L., Buratti, E., Baralle, F., de Belleroche, J., Mitchell, J. D., Leigh, P. N., Al-Chalabi, A., Miller, C. C., Nicholson, G., and Shaw, C. E. (2008) TDP-43 mutations in familial and sporadic amyotrophic lateral sclerosis. *Science* **319,** 1668–1672

78. Jao, D. L., and Chen, K. Y. (2006) Tandem affinity purification revealed the hypusine-dependent binding of eukaryotic initiation factor 5A to the translating 80S ribosomal complex. *J. Cell. Biochem.* **97,** 583–598

79. Strong, M. J., Volkening, K., Hammond, R., Yang, W., Strong, W., Leystra-Lantz, C., and Shoesmith, C. (2007) TDP43 is a human low molecular weight neurofilament (hNFL) mRNA-binding protein. *Mol. Cell. Neurosci.* **35,** 320–327

80. Ou, S. H., Wu, F., Harrich, D., García-Martínez, L. F., and Gaynor, R. B. (1995) Cloning and characterization of a novel cellular protein, *TDP-43,* that binds to human immunodeficiency virus type 1 TAR DNA sequence motifs. *J. Virol.* **69,** 3584–3596

81. Tanaka, N., Kyuuma, M., and Sugamura, K. (2008) Endosomal sorting complex required for transport proteins in cancer pathogenesis, vesicular transport, and nonendosomal functions. *Cancer Sci.* **99,** 1293–1303